Updated Review of the Life and Reliability Models for HVDC Cables

Giovanni Mazzanti, *Fellow, IEEE*

Abstract— **This article updates previous reviews of life and reliability models for high-voltage direct-current (HVDC) cables. The update is motivated by the impressive research and development activities on HVDC cable systems in the last years, with many projects at increasing levels of voltage and power; this makes the sound evaluation of the life and reliability of HVDC cables crucial. Physical and phenomenological life models proposed over the years for constant electrical and thermal stresses are reviewed first, including the relevant probabilistic framework and the effects of cable insulation volume enlargement. Then, more recent procedures for life and reliability estimation under time-varying electro-thermal stress are reported, focusing on thermal transients due to load cycles and voltage transients due to long temporary over-voltages (TOVs), superimposed switching impulses (SSIs), and voltage polarity reversals (VPRs). Results of the application of such procedures are also presented, with a discussion on their limitations and open issues.**

Index Terms— **Extruded insulation, high voltage direct-current (HVDC) cables, lapped insulation, life models, power system transients, reliability.**

I. INTRODUCTION

IN THE last years, the huge research and development activities on high voltage direct-current (HVDC) cable systems—especially of the extruded type [1], [2]—have led to many HVDC cable link projects realized or planned at increasing levels of voltage and power, e.g., the German Corridors, three ±525 kV-dc/2 GW extruded cable lines from offshore wind farms in the North Sea to industrial areas in South Germany [3]; or the Western Link, a ±600 kV-dc/2.2 GW paper-poly-propylene laminated (PPL) cable line connecting England to Scotland [4]. Such challenging targets of voltage and power make the sound evaluation of the life and reliability of HVDC cables a crucial issue. This issue is under the spotlight also in the European Union (EU) H-2020 NEWGEN research project, aiming at a new generation of HVDC insulation materials, cables, and systems [5]; indeed, the tasks of the project include both refining existing life and reliability models of HVDC cables and developing new ones capable of treating the many transient conditions faced in service by cable systems.

In this respect, let us point out that life and reliability models serve three key purposes in cable research and development, namely [6]:

1) Comparing different insulation compounds to choose the best for its endurance to applied stresses.
2) Choosing durations and stress levels for voltage tests, in particular, the prequalification test (PQT), the extension of qualification test (EQT), and the type test (TT) [7], [8], [9], [10], [11].
   a) Estimating life in service, to choose cable insulation design parameters (geometry, thickness, and stress levels).

However, many issues arise in achieving these goals, in particular the last one. Three examples are as follows:

1) Possible changes in aging mechanisms make it difficult—or even impossible—to achieve a general model valid whichever the stress levels, as the degradation and failure mechanisms valid for the high stresses of accelerated life tests (ALTs) might not be valid at service stresses.
2) Life models generally assume that applied stresses are controlled and do not vary during cable life, as it occurs during ALTs. On the contrary, service stresses on HVDC cable insulation are not constant, first and foremost due to changes in load current and voltage transients [6], [12].
3) Breakdown field/voltage changes with the size of the insulation, as the larger the insulation volume, the greater the number and dimension of imperfections from which degradation and breakdown generally stem.

In [13] and [14], general reviews of life models for electrical insulation to be used under ac and dc voltage were given. In [15], a first review of life models for HVDC extruded cables was provided, treating the main life models for HVDC extruded cable insulation under constant electrical and/or thermal stress associated with the role of trapped space charge. In [6, Ch. 6], a more general review of life and reliability models that can be used for HVDC extruded cables was provided, further broadened in [16] with the treatment of load cycles and of the enlargement of insulation volume from test minicables to full-size cables.

This article aims at updating the reviews in [6], [15], and [16] by doing the following:

1) Including some models omitted there for brevity.
2) Introducing novel models developed in more recent years.
3) Extending the review to include lapped HVDC cables.

The article is organized as follows. In Section II, the basics of life and reliability modeling of HVDC cables are recalled. In Sections III and IV, physical and phenomenological life models, respectively, under constant electrical and thermal stresses are reviewed. In Section V, a probabilistic framework for electro-thermal life models at constant stresses is given under the Weibull hypothesis. In Section VI, the effects of the enlargement of HVDC cable insulation volume are treated. In Section VII, a procedure for life and reliability estimation under the thermal transients due to load cycles is illustrated. In Section VIII, a procedure for life and reliability evaluation under-voltage transients is described, focusing on long temporary over-voltages (TOVs), superimposed switching impulses (SSIs), and voltage polarity reversals (VPRs); some applications of these procedures are also reported. Section IX discusses the limitation of these tools. Section X points out open issues.

II. FUNDAMENTALS OF LIFE AND RELIABILITY MODELING OF HVDC CABLES

The "life model" of a power cable is a mathematical relationship between the time-to-failure—or "life"—of cable insulation (the weakest part of a cable) and the levels of applied stresses [6], [13], [14], [15], [16]. Indeed, applied stresses "age" cable insulation, i.e., progressively and irreversibly degrade its dielectric properties until failure or "electrical breakdown." This latter consists of a perforation of the insulation wall, whose breakdown strength cannot be restored [6], [13], [14].

The breakdown is almost instantaneous when the applied stresses are very high, but in service, it is mostly the ultimate result of a long and random aging process, since the time-to-failure increases as the stress level decrease [6], [13], [14]. Hence, the study of the main stresses and of their effect on the dielectric is fundamental in power cable insulation life modeling. For HVDC cable insulation, the main stresses on duty are [6], [12], [16].

1) Electric stress E', caused by voltage and evaluated quantitatively as the electric field strength.
2) Thermal stress T', caused by temperature and evaluated quantitatively in the form of a conventional thermal stress.
3) Mechanical stress M', caused e.g., by tension, coiling, bending, vibration, and expansion/compression.
4) Ambient stress A', associated with aging factors in the laying environment, e.g., humidity, corrosion, and UV radiation.

Life model parameters are derived empirically either from dedicated chemical-physical measurements or—more often—from the life versus stress results of ALTs [17] done at higher-than-rated stresses, to make ALT last much less than the design life of the insulation (40 years for HVDC cables) [7], [8], [9]. The more the applied stresses, the harder is to perform the ALT campaign, as well as evaluate model parameters accurately and confidently.

Electrical and thermal stress plays a major role in cable design, testing, and service, as they always occur in cables on duty. Thus, most if not all life models for HVDC cables

found in the literature fall into one of the three following classes [6], [15], [16]:

1) Single-stress electrical life models. Here the only applied stress is the voltage/electric field.
2) Single-stress thermal life models. Here the only applied stress is temperature.
3) Combined electro-thermal life models. Here the applied stresses are voltage/electric field and temperature.

Reliability is inherently correlated with life models, as aging and breakdown are random phenomena ruled by stochastic laws. This is due to the intrinsic nonuniformity of the insulation, which makes macroscopic degradation the result of manifold degradation processes occurring at the microscale in a more or less nonuniform and random way: charge injection, transport, and storage; dielectric losses; field enhancement at sharp conducting points; overheating at conductor/insulation interface; partial discharges (PDs) in voids; water treeing; Maxwell forces; and thermo-mechanical stresses; etc. [18]. Hence, time-to-breakdown is always associated with a certain failure probability F, or reliability $R = 1 - F$. By assuming a proper probability distribution for times-to-failure, the life model is turned into a comprehensive probabilistic life model (or reliability model) capable of predicting the relationship between life, applied stresses and cumulative failure probability—or reliability [6], [17], [19], [20].

Sections III and IV review life models for HVDC cables under constant electrical and thermal stress, split into two classes [16]:

1) Physical or microscopic life models, assuming that the main source of degradation is aging associated with local microdefects, and aiming at explaining such aging.
2) Phenomenological, empirical, or macroscopic life models, relying solely on ALT results as a global output of the various aging mechanisms and aiming simply at the attainment of an empirically-satisfactory relationship between life and applied stresses.

III. PHYSICAL LIFE MODELS

As hinted at before, physical life models focus on local micro-imperfections in the insulation as the cause of aging. Generally physical life models stem from an aging model, which tries to describe the chemical-physical processes of local degradation to predict life as the time of a critical level of aging; this critical level makes the insulation unable to perform satisfactorily, thus causing breakdown [6], [15], [16], [18]. Another typical feature of physical life models is that they mean life as the inception-time of electrical treeing, regarding treeing-growth-time to break-down as negligible versus treeing-inception-time [6], [15], [16]. For this reason, the treeing growth models found in the literature [21], [22] are skipped here, although treeing-growth-time might be important for high electric fields and/or large defects.

Most physical life models are developed for polymeric cable insulation and address aging and breakdown of the insulation to the polymer structure, with amorphous regions not full of atoms or molecules [18], [23], [24], [25], [26], [27]. The unfilled part of the amorphous phase consists of free volume, i.e., small empty spaces between the molecules, where free
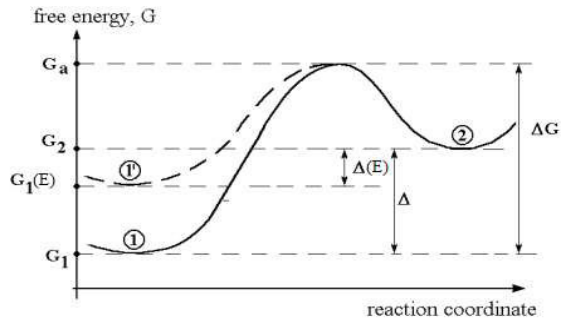
Fig. 1. Free energy diagram in the absence (solid line) and in the presence (dashed line) of electric field. After [29].

charge carriers may gain energy from the field, thereby starting degradation processes [24], [26], [27]; also, the insulation may feature microvoids present since manufacturing, or created by bulk aging processes. On these grounds, the main classes of physical life models for HVDC cable insulation are singled out from the different aging processes addressed by the various models, as follows [15], [16]:

1) Thermodynamic models [28], based on local mechanical stresses or strains that modify the activation energy of chemical-physical degradation reactions.
2) Space-charge-based models, stemming from the previous ones, but with particular emphasis put on local space charge centers as a source of chemical-physical aging.
3) Models based on PD-induced damage growth from microvoids present in the insulation since manufacturing.

A. Thermodynamic Models

Thermodynamic models regard electrical degradation under voltage/field and temperature as a thermally-activated aging phenomenon [6], [28], where the summary is as follows (see Fig. 1 after [29]):

1) An activation free energy barrier ΔG has to be overcome to turn the insulation from an unaged state ($=$ free energy G_1) to the aged state ($=$ free energy G_2).

2) The electric field lowers the free energy barrier ΔG by storing electromechanical energy locally, thus leading to the onset of a field-dependent barrier-lowering term.

The main thermodynamic models that can be used for HVDC cable insulation are as follows:

1) *Endicott model* [30], obtained from the single-stress thermal Eyring model (see Section IV-B) by introducing an ad hoc field-dependent free energy barrier. The model is as follows:

$$L(E, T) = C_E T^{-w} \exp[\Delta G/(k_B T)] \exp[-(k_1 + k_2/T)E]$$
(1)

where $L(E, T)$ is the "electro-thermal" life of the insulation, function of electric field strength E and absolute temperature T; k_B is Boltzmann's constant; C_E is a parameter depending on the dielectric, as well as—often—on E and T; w, k_1, and k_2 are quantities mainly characteristic of the dielectric [6], [15], [30].

2) *Lewis model* [31], [32], [33], based on the hypothesis that electromechanical stress causes degradation by enlarging

small microcavities present since manufacturing, until electrical trees—the final stage of aging—are triggered. In turn, electrical trees are regarded as "cracks," whose propagation is described via the Griffith crack theory. Life is meant as the time to start crack propagation, t_C, hypothesized to be by far the longest time interval of the total aging duration, thus well approximating the whole time-to-failure; t_C has the following expression:

$$t_C = \int_{N_b}^{\eta_C} \left\{ \frac{k_B T}{h_P} \left[\exp\left(\frac{-G_b(E)}{kT}\right)(N_b - \eta) \right. \right.$$
$$\left. \left. - \exp\left(\frac{-G_f(E)}{k\Theta}\right)\eta \right] \right\}^{-1} d\eta$$
(2)

where h_P is Planck constant; G_f and G_b are the energies for bond forming and breaking, respectively (linked to G_1 and G_2 in Fig. 1); N_b is the number of breakable bonds; η is the number of broken bonds, whose critical value is η_C [6], [31], [32], [33].

Lewis model exhibits a field threshold below which no aging takes place and life tends to infinity. Space charge effects were introduced later in the model with a focus on polyethylene (PE) under electric stress. For more details—omitted for brevity—see [33].

3) *Crine model* [34], [35], obtained from concepts similar to the Lewis model under the following assumptions.

1) The applied electric field causes electro-mechanical stress straining van der Waals' bonds between polymer chains included in a proper activation volume ΔV. Thus, the submicro- or nano-cavities already present within ΔV are widened and insulation is degraded until failure.
2) Degradation proceeds as a competition between a forward and a backward reaction, both partly reversible.
3) The electromechanical energy lowers the activation-free energy barrier of insulation degradation, ΔG, thereby fostering the aging mechanism.

Electro-thermal life according to the Crine model is given as

$$L(E, T)$$
$$= [h_P/(2k_B T)] \exp[\Delta G/(k_B T)] \operatorname{csch}[(1/2)\varepsilon \Delta V E^2/(k_B T)]$$
(3)

where ε is the permittivity of the dielectric. More details—omitted for the sake of brevity—can be found in [34] and [35].

B. Space Charge-Based Models

The so-called Dissado-Mazzanti-Montanari (DMM) aging and life model has a thermodynamic basis and is perhaps the first physical life model where space charges trapped in the insulation have a main role in aging and failure of dc extruded cable insulation [29], [36], [37]. Its main assumptions are as follows:

1) Since manufacturing the insulation of HVDC cables is affected by spherical micro- or nano-voids of radius r_V.
2) Such voids are regarded as space charge storage centers, capable of storing an amount $q_C = C_q E^{b_q}$ of space charge, where C_q, b_q are parameters related to the space charge accumulation features of the dielectric [29], [38].

3) At space charge storage centers, the Poissonian field associated with space charge predominates over applied field E associated with dc voltage.

4) Each center degrades N_m microstructural units, referred to as "moieties"—e.g., inter/intra-chain bonds, cross-linking bonds in cross-linked polymers, etc.—located within a shell of a thickness λ on the void boundary.

5) Degradation proceeds as a competition between a forward and a backward reaction, both partly reversible.

6) The conditions for breakdown take place locally as soon as the fraction of degraded moieties, A, exceeds a critical value, A^*, which depends on the dielectric. This triggers an electrical tree that brings insulation to failure very soon. In this framework, time-to-failure ($=$ life) is regarded as the time to electrical tree triggering.

By developing these hypotheses, the electro-thermal life $L(E, T)$ according to the DMM model is obtained as follows:

$$L(E, T) = \frac{h_P}{2k_B T} \exp\left(\frac{\Delta H/k_B - C'E^{2b_q}/2}{T} - \frac{\Delta S}{k_B}\right)$$
$$\times \ln\left[\frac{A_{eq}(E)}{A_{eq}(E) - A^*}\right]\left[\cosh\left(\frac{\Delta/k_B - C'E^{2b_q}}{2T}\right)\right]^{-1} \tag{4}$$

$$A_{eq}(E) = 1/\{1 + \exp[(\Delta/k_B - C'E^{2b_q})/T]\} \tag{5}$$

$$C' = (B_q \alpha_E \delta_S \lambda C_q^2)/(16\pi \varepsilon^2 r_V^2 N_m k_B) \tag{6}$$

where ΔH is the activation enthalpy per moiety; ΔS is the activation entropy per moiety; Δ is the free energy difference between unaged (or "reactant") and aged (or "degraded") state; $A_{eq}(E)$ in (5) indicates the value of A at the equilibrium between forward reaction and backward reaction; C' in (6) is a constant typical of the dielectric, being $B_q =$ proportionality constant between the stored electromechanical energy per moiety and its contribution to the free energy barrier of degradation, $\alpha_E =$ electrostriction coefficient, $\delta_S =$ elemental strain [36], [37].

The DMM model features an electrical threshold—i.e., a field level below which electrical aging is absent and life tends to infinity—in agreement with the threshold for space charge accumulation demonstrated in polymeric insulation [38]. The DMM was shown in [37] to fit satisfactorily ALT results carried out at 20 °C under dc voltage on 0.15 mm plaques of cross-linked polyethylene (XLPE) for HVDC cables (dc-XLPE), and to provide results in fairly good agreement with dc life tests reported in [39]. More details—omitted here for the sake of brevity—appear in [15], [29], [36], and [37]. More recently in [40] and [41], the DMM life model enabled a new way of inferring the life of full-size cables from ALTs on thin laboratory samples, as hinted at in Section VI.

After the DMM model, a more recent physical space charge-based life model focused on polymeric insulation was proposed in [24] and [27] by emphasizing the link between manufacturing features in polymers (e.g., free volume, submicrovoids, and low-density regions) and charge trapping/detrapping processes. Here are the hypotheses on which this "trapping/detrapping" space charge-based model relies [24], [27].

$$t_C(E, T) = \left[\frac{\sigma_T}{q_e}AT^2 \exp\left(-\frac{\Phi - \beta_s E^{1/2}}{k_B T}\right)\right.$$
$$\left. + N_c v_{th} \sigma_T \exp\left(-\frac{G_t - W_{em}}{k_B T}\right)\right]^{-1}$$
$$+ \ln\left[\frac{C - C_0}{C - C^*}\right] \tag{7}$$

1) The polymeric insulation of HVDC extruded cables has a mixed crystalline/amorphous structure made up of many moieties. Due to the inherent nonhomogeneity of polymers, different properties hold for each moiety.

2) The amorphous phase features free volume and empty spaces where injected electrons travel easier than in the crystalline phase, gaining energy over a free path under the applied electric field similarly as in gases [42].

3) Charge dynamics during electro-thermal aging is defined by trapping and detrapping of electrons in the free volume, according to a set of kinetic equations reported in [24] and [27]—based on empirical trapping and detrapping coefficients, K_T and K_D.

4) As for trapping rate, an experimental investigation of current density versus electric field indicates the Schottky injection as the appropriate mechanism for low-density polyethylene (LDPE) films, which the model focuses on.

5) As for the detrapping rate, thermal detrapping is considered, occurring when the trapped charge carrier gains its energy for detrapping from thermal lattice vibrations. Thermal detrapping is further adjusted to include the trap energy-lowering effect of the electromechanical energy W_{em} associated with the storage of space charge in the trap, related in turn to the electric field.

6) Life $t_C(E, T)$ never ends until the fraction of trapped charges $X(t)$ reaches a critical value C^* such that the released electromechanical energy from detrapping can break the insulation bonds, leading to failure. Hence, the life model is obtained by setting $X(t_C) = C^*$ in the kinetic equations integrated over $t_C(E, T)$, which gives

where $\sigma_T =$ capture cross section, $A =$ Richardson–Dushman constant, $q_e =$ electron charge, $\Phi =$ height of electrode-insulation barrier, $\beta_s = (q_e/4\pi\varepsilon_r\varepsilon_0)^{1/2}$, $N_c =$ effective density of states in the conduction band, $v_{th} =$ thermal speed of charges, $G_t =$ trap depth, $C =$ equilibrium value of X, and $C_0 =$ initial value of C [24], [27].

The life model (7) has the good feature that, apart from C^*, its parameters can come from other investigations than ALTs; in [27] it fit satisfactorily the results of electro-thermal ALTs on LDPE samples under dc voltage at 80 °C (see Fig. 2).

C. Model Based on PD-Induced Damage Growth

A physical electro-thermal life model was proposed in [43] and [44], which addresses the degradation of HVDC PE-based cable insulation to the appearance of PDs within microcavities that are present since manufacturing. The main hypotheses on which this model relies are as follows:
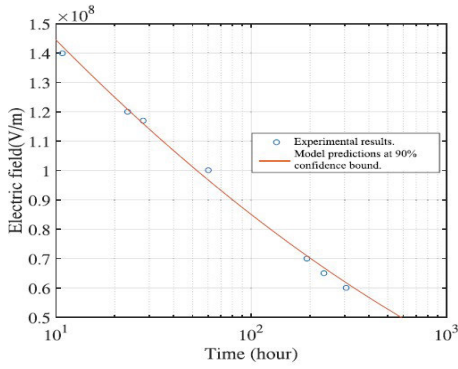
Fig. 2. Life line from (7), fitting 63.2%-ALT results relevant to LDPE samples under dc voltage at 80 °C. After [27].

1) HVDC PE-based cable insulation features air-filled microvoids, roughly assumed as cylindrical of radius R, circular base S, and height d along the field direction.
2) Electrons injected from the electrodes or already in the insulation bulk are carried through the polymer via thermally activated hopping and eventually reach the PE-void interface, where the negative electron affinity of PE fosters charge trapping. Then, trapped electrons are injected into the void through the Schottky effect.
3) Hot-electron avalanches start from the PE-void surface and impinge on the opposite void-PE surface.
4) At this surface, the PE matrix is damaged due to the rupture of CH bonds, and a degraded "pit" grows with time until it reaches a critical size d_C. Then it triggers an electrical tree, thus bringing insulation quickly to failure.

From the above assumptions, the degradation process until the breakdown is explained in the three following steps [43], [44]:

1) Injection of electrons into the cavity at PE-cavity surface. This step yields the electron injection rate, R_{inj}.
2) Development of electron avalanches in the void. This step yields the electron energy distribution, highlighting.
   a) The "hot" fraction F_{hot} of electrons that overcome the bond-breaking energy of CH bonds, is equal to 8 eV.
   b) The "effective" fraction F_{eff} of electrons that in fact break CH-bonds in a statistical sense.
   c) The number of electrons impinging the void-PE surface, $R_{\text{el}} = R_{\text{inj}} N_{\text{el}}$, where N_{el} is the number of electrons generated in the cavity from one injected electron.
3) Growth of degradation from the void-PE surface into the polymer lattice. This step yields.
   a) t_{dis} = time-to-disruption of a slab of thickness D_{dis} with a number N_{CH} of CH-bonds exposed to damage.
   b) R_{dis} = degradation growth rate in the polymer lattice.
   c) $L(E, T)$ = electro-thermal life, meant as the time to attain a critical size d_C of the degraded region.

The main equations of the model are thus the following:

$$R_{inj} = \frac{J_C S}{q_e k_B T} \frac{2q_e^2}{4\pi \varepsilon_0 R}$$
$$\times \left\{ \ln\left[1 + \frac{2q_e^2}{4\pi \varepsilon_0 R k_B T} \right.\right.$$
$$\left.\left. \exp\left(\frac{G_t - q_e((q_e \varepsilon_r E)/(4\pi \varepsilon_0))^{1/2}}{k_B T} \right) \right] \right\}^{-1}$$
(8)

$$t_{dis} = N_{CH}/(2R_{el}F_{eff}F_{hot}) = N_{CH}/(2R_{inj}N_{el}F_{eff}F_{hot})$$
(9)

$$R_{dis} = D_{dis}/t_{dis}$$
(10)

$$L(E, T) = d_C/R_{dis}$$
(11)

where J_C = conduction current density. For details, see [43].

In [44], this model with $d = 27$ μm, $d_C = 3$ μm fit well the failure times at 20 °C from dc XLPE cable tests after [39].

IV. PHENOMENOLOGICAL LIFE MODELS

Phenomenological life models for dc cable insulation under constant stresses look like life models for ac cable insulation, the main difference being the values of model parameters. The general form of such phenomenological life models is

$$L = L(S_1, \ldots, S_N)$$
(12)

where L is life; $S_1, \ldots, S_N$ is a set of N applied stresses, taken as constant with time, among which the electrical and thermal stresses are the key ones in HVDC cable design, development, and testing (see Section II). Thus, most—if not all—phenomenological life models for HVDC cable insulation found in the literature are single-stress thermal and electrical, and combined electro-thermal life models, as described hereafter [6], [14], [16].

A. Single Stress Electrical Life Models

The simplest and most popular phenomenological life model for HVDC cable insulation is the electrical inverse power model (IPM) or V–t characteristic [6], [7], [9], [14], [15], [16], [17], [39], [45], which—as witnessed by these names—expresses insulation life t (or t_F, or L) as an inverse power of applied voltage V or U—or of electric field E—as follows:

$$U^n t = \text{constant}$$
(13)

where n is the so-called life exponent [6], [39], [45].

Equation (13) is used by manufacturers for designing high voltage alternating current (HVAC) and HVDC cables [39], as well as by International Standards for attaining the duration t_1 and the voltage level U_1 of loading cycle voltage tests for the qualification of HV cables. t_1 and U_1 come from (13) applied to design life L_0 at rated voltage U_0 and to test duration t_1 ($\ll L_0$) at test voltage U_1 ($\gg U_0$) [6]. Then

$$t_1 = L_0(U_1/U_0)^{-n}.$$
(14)

In (14): IEC 62 067 [11] assumed implicitly $n = 7$ to set the duration and voltage of the PQT on EHVAC extruded cables;

TABLE I
DERIVATION OF PQT VOLTAGE U_1 ACCORDING TO [11] FOR EHVAC EXTRUDED CABLES, TO [9] FOR HVDC EXTRUDED CABLES, AND TO [10] FOR HVDC LAPPED CABLES

Cable type	Standard	rated life L_0 [y]	duration t_1 [d]	n	PQT voltage U_1 (p.u. of U_0)
AC extrud.	IEC 62067	40	365	7	$\sqrt[7]{40\times365/365}=1.7$
DC extrud.	TB 852	40	360	10	$\sqrt[10]{40\times365/360}=1.45$
DC lapped	TB 853	40	360	11	$\sqrt[11]{40\times365/360}=1.4$

Cigrè Technical Brochure (TB) 496:2012 first [7], and later IEC 62 895 [8] and TB 852:2021 [9] assumed explicitly $n = 10$ to set the durations and voltages of PQT, EQT, and TT on HVDC extruded cables; TB 853:2021 [10] assumed implicitly $n = 11$ to set the durations and voltage of PQT on HVDC lapped cables.

Table I lists the PQT voltages in [9], [10], and [11]. Clearly, n depends on the voltage waveform and insulation features. ALTs done on last-generation dc-XLPE provide values of n ranging from ≈ 15 up to ≈ 20 or more [46], [47], hence the value of $n = 10$–11 after [7], [9], [10] seems underestimated. A more careful inspection of results reveals that n depends also on temperature [14] (see below), with a tendency to lower values of n as temperature increases, despite some contrasting results, particularly at temperatures only moderately higher than the room [48].

When comparing (12) with (13), (14) it can be understood that the IPM is obtained from (12) by setting $N = 1$, $S_1 =$ electric stress $= E'$, which is given by applied voltage U in (13) and (14); hence the IPM belongs to the class of single-stress electrical life models. More often in the literature E' is represented through local electric field strength E, to account properly—as physical life models emphasize—for the most stressed location in the insulation, where the critical conditions for breakdown will be likely reached first (although this is not 100% granted due to insulation inhomogeneity [40], see Section IX). For instance, replacing U with E and assuming as a reference field either the highest test electric field E_H (typically $E_H = E_B =$ breakdown strength), or the much lower rated electric field E_0, two alternative forms of the IPM are obtained, respectively [6]

$$L(E) = L_H(E/E_H)^{-n} \tag{15}$$
$$L(E) = L_0(E/E_0)^{-n} \tag{16}$$

where $L_H = L(E = E_H)$ is the value of L at reference electric field E_H and $L_0 = L(E = E_0)$ is the value of L at reference electric field E_0, being $L_0 \gg L_H$ as $E_0 \gg E_H$. Sometimes E_0 denotes a field value under which the electrical aging is negligible [14].

As detailed in [16], from (15) to (16) let us consider two insulations 1 and 2 with $n_2 > n_1$ and the same value of breakdown strength E_H, obtained after the short test time L_H: at the rated field E_0, the life of insulation 2, $L_0(2)$, is longer than the life of insulation 1, $L_0(1)$, since $n_2 > n_1$, thereby explaining why n is also called voltage endurance coefficient (VEC) [6], [14].

Other phenomenological electrical life models were suggested for HVDC cable insulation—e.g., the exponential

model without or with an electrical threshold, the IPM with an electrical threshold [14], [15]—but threshold models give a poorer safety margin than no threshold models. However, other phenomenological electrical life models are skipped here both for brevity and since the IPM.

1) Is the reference electrical life model for the main International Standards on HVDC cables [7], [8], [9], [10].
2) Is the most employed for HVDC cable insulation due to its simplicity and flexibility in fitting the various electrical ALTs on dielectrics for dc cable insulation [14], [15], [16], [17], [45], [46], [47], [49].
3) Is theoretically founded on a statistical approach relying on the Weibull probability distribution [50] (see Section V).

B. Single Stress Thermal Life Models

Single stress phenomenological thermal life models refer to the case when (absolute) temperature T is the only stress applied to HVDC cable insulation; then in (12) $N = 1$, $S_1 = T'$ (thermal stress, depending on T) and $L(S_1, \ldots, S_N)$ reduces to $L(T)$.

The most popular thermal life model in the literature—not only for HVDC cable insulation, but for electrical insulation in general—is the Arrhenius thermal life model [14]. This is not simply a phenomenological thermal life model—since it fits well with the results of ALTs with temperature as the only applied stress for a wide variety of materials and over a broad range of temperatures [51]—but it can also be seen as a physical life model. Indeed, according to Dakin's theory [52], temperature speeds up exponentially the rate of thermally-activated chemical degradation reactions of dielectrics, first and foremost oxidation, but also de-polymerization, hydrolysis, and cross-linking [18]. Assuming that one main degradation reaction exists—with activation energy ΔW—for the dielectric over the considered temperature range, the following general expression of the Arrhenius thermal life model is attained [14], [52]:

$$L(T) = R_T \exp[\Delta W/(k_B T)] \tag{17}$$

where R_T is a material-dependent constant, inversely proportional to the reaction rate constant [6], [14].

Similar to the IPM, by taking as a reference either the maximum test temperature T_H, or a much lower temperature T_0 (typically the rated temperature of cable insulation, or the room temperature), two alternative and more manageable expressions of the Arrhenius model are obtained, respectively,

$$L(T) = L_H \exp[-B(1/T_H - 1/T)] = L_0 \exp(-B\,T'') \tag{18}$$
$$L(T) = L_0 \exp[-B(1/T_0 - 1/T)] = L_0 \exp(-B\,T') \tag{19}$$

where $B = \Delta W/k_B$; $L_H = L(T = T_H) = L_0 \exp[-B(1/T_0 - 1/T_H)]$ is the value of L at reference temperature T_H; $L_0 = L(T = T_0)$ is the value of L at reference temperature T_0; $T' = 1/T_0 - 1/T$ or $T' = 1/T_H - 1/T$ are two alternative expressions of the so-called conventional thermal stress [16].

Relying on the Arrhenius model, IEC Standard 60 216 provides guidelines on the estimation of the thermal endurance of a dielectric from the results of ALTs at constant T [51].

This is done via the so-called Arrhenius graph, a plot whose coordinates are log(life) versus $-1/T$, whereby the Arrhenius model life line according to both (18) and (19) becomes a straight line of slope $-B$; starting from test temperature T_H such line can be extrapolated to rated or room temperature T_0, thus attaining [51].

1) The temperature index (TI), that is the Celsius temperature yielding a life of 20 000 h.
2) The halving interval in Celsius (HIC), that is the temperature rise from the temperature of TI yielding a life of 10 000 h, i.e., half of the life at the TI.

Another thermal life model is the physical Eyring model [53], brought back from the previous Endicott model (1) when setting $E = 0$, $w = 1$, and $C_E = h_P/k_B$ [14], [15]

$$L(T) = h_P/(k_B T)\exp\left[\Delta G/(k_B T)\right]. \qquad (20)$$

The Eyring model provides the TI and HIC like the Arrhenius model, but—as the values of TI and HIC given by the Eyring and Arrhenius models differ only slightly [13], [16]—the latter is chosen by [51], being simpler than the former.

C. Combined Electro-Thermal Life Models

If both voltage U and temperature T are applied, in (12) $N = 2$, $S_1 = E'$ (electric stress), $S_2 = T'$ (thermal stress), and $L(S_1, \ldots, S_N)$ turns to $L(E', T')$. In the literature for HVDC cable insulation $L(E', T')$ is often obtained by merging the IPM electrical model as per (16)—then $E' = E =$ electric field strength—with the Arrhenius thermal model as per (19)—then $T' = 1/T_0 - 1/T$. In this way, the so-called IPM-Arrhenius electro-thermal life model is derived, which can be written as [14], [54], [55], [56]

$$L(E, T) = L_0(E/E_0)^{-\left(n_0 - b_{ET} T'\right)} \exp\left(-B\,T'\right) \qquad (21)$$

where $L_0 = L(E = E_0, T = T_0) =$ life at reference electric field E_0 and temperature T_0; $n_0 =$ VEC at reference temperature T_0; $b_{ET} =$ parameter ruling the synergism between electrical and thermal stress [14], [54], [55].

Another equivalent expression of the IPM-Arrhenius model is obtained by introducing in (21) the design electric field, E_D, the design temperature, T_D, and the design life, L_D, of the cable, thereby arriving at the following equation reported in [57]:

$$L(E, T) = L_D[E/E_D]^{-(n_D - b_{ET} T_d)}\left[E_D/E_0\right]^{b_{ET} T_d} e^{-BT_d} \qquad (22)$$

where $T_d = 1/T_D - 1/T$, $n_D =$ VEC at design temperature T_D.

Other electro-thermal life models were proposed for HVDC cable insulation, stemming from the electrical exponential model without or with an electrical threshold [6], [14]. Thus, a more general and comprehensive form of the electro-thermal life model for HVDC cables was reported in [54], namely

$$\begin{aligned} L(E, T) \\ = L_0 \exp(-n_0 E'' - BT' + b_{ET} E'' T')/[E''/E_t''(T) - 1]^\mu \end{aligned} \qquad (23)$$

where the generalized electric stress $E'[U + 2033]$ appears instead of field strength E; $E'[U + 2033]$ can be either $E'[U + 2033] = E - E_0$ or $E'[U + 2033] = \ln(E/E_0)$: in the

former case (23) yields the "exponential-Arrhenius" electro-thermal model [14] (neglected here for brevity), in the latter case the IPM-Arrhenius model (21) [6], [16], [54], [55], [56]. $E'[U + 2033]_t(T)$ is the electrical threshold, i.e., the electric stress value below which—if any—cable life tends to infinity at temperature T; μ is an exponent equal to zero if a threshold is not detected.

In fact, the threshold $E'[U + 2033]_t(T)$ can be guessed: for HVDC lapped cables from service experience especially on mass-impregnated nondraining (MIND) cables, for which various dissections showed no drop of breakdown strength after 30–50 years of service, and failures were due almost only to external factors [58]; for HVDC extruded cables from space charge, electro-luminescence and electrical conductivity measurements on dc polymeric insulation, which indicate a threshold field in the range 10–20 kV/mm [38], [59], [60].

As readily seen from the previous treatment of the IPM and Arrhenius life models, the IPM-Arrhenius can be deemed as the most popular and viable phenomenological electro-thermal life model for HVDC cable insulation for the following reasons:

1) The IPM and the Arrhenius life models are, respectively, the reference electrical and thermal models of International Standards for HVDC cable insulation [7], [8], [9], [10], [51].
2) The IPM and the Arrhenius life models are simple and flexible, so as to fit satisfactorily ALT data for various HVDC cable-insulating compounds tested with different fields, temperatures, and test cells. Such flexibility is transferred to their combination, namely the IPM-Arrhenius electro-thermal life model [6], [16], [54], [55], [56].

The IPM model (16) and the Arrhenius model (19) feature two parameters, i.e., L_0, n and L_0, B, respectively, whereas their combination—i.e., the IPM-Arrhenius (21)—features four parameters, i.e., L_0, n_0, B, b_{ET}, whose evaluation is more difficult and uncertain than for the parameters of single-stress models.

V. PROBABILISTIC FRAMEWORK OF LIFE MODELS FOR HVDC EXTRUDED CABLE INSULATION: THE RELIABILITY MODELS

Electrical insulation is inherently nonhomogeneous. Even the macroscopically-uniform matrix of polymeric dielectrics for HVDC extruded cables has imperfections such as voids, contaminants, and semicon protrusions [6], [9], [61]; defects (e.g., irregularities in tape layout, in butt gaps size and shape, etc.) are found also in lapped cables, whose in-homogeneity is more evident due to their macroscopic multilayered structure [10], [12]. Thus, the breakdown process of HVDC cable insulation is a random phenomenon ruled by stochastic laws, and time-to-failure has always been associated with a certain failure probability [6], [17], [18], [19], [20]. For the insulation of HVDC cables, the two-parameter Weibull probability distribution is generally assumed to describe the relationships between [6] and [16] as follows:

$$P_B = 1 - \exp[-(E_B/\alpha_E)^{\beta_E}] \qquad (24)$$

$$P_F = 1 - \exp[-(t_F/\alpha_t)^{\beta_t}]. \qquad (25)$$

1) The random variable breakdown strength, E_B, and the cumulative probability of breakdown, P_B, see (24).
2) The random variable time-to-failure (i.e., life), t_F, and the cumulative probability of failure, P_F, see (25)

where β_E is the shape parameter of the probability distribution of breakdown strength E_B, and α_E is the 63.2th percentile of E_B (or the scale parameter of its distribution); β_t is the shape parameter of the probability distribution of failure time t_F, and α_t is the 63.2th percentile of t_F (or the scale parameter of its distribution).

Weibull cumulative probability distributions (24) and (25) yield straight lines in $\log[-\ln(1 - P_B)]$ versus $\log(E_B)$ and $\log[-\ln(1 - P_F)]$ versus $\log(t_F)$ coordinates, respectively—also called Weibull charts or plots [17]. Their combination led long ago [62], [63] to the so-called "two-variables" or "generalized" Weibull distribution, $P(E_B, t_F)$, which reduces to (24) at constant time t_F and to (25) at constant breakdown strength E_B, i.e., [64]

$$P(E_B, t_F) = 1 - \exp\left[-\gamma E_B^{\beta_E} t_F^{\beta_t}\right]. \tag{26}$$

From (26) at a given and constant probability P one obtains

$$E_B^{\beta_E} t_F^{\beta_t} = \text{const.} \tag{27}$$

That is, the IPM of (13) with $n = \beta_E/\beta_t$, $E_B = E \ (\propto U)$ and $t_F = t$. However, in [64], the generalized Weibull distribution was discarded claiming an inconsistency in the derivation of the two "partial" distributions of E_B and t_F whose combination yields (27); indeed, the distribution of E_B comes from short-term rising voltage tests until failure, while the distribution of t_F comes from constant voltage tests until failure [17], [50], [64].

Let us note that in general α_t in (25) depends on the applied stresses, thus here electrical stress E' and thermal stress T'. Then, $\alpha_t = \alpha_t(E', T')$ and (25) can be rewritten as follows:

$$P_F = P(t_F, E, T) = 1 - \exp\left\{-\left[t_F/\alpha_t(E', T')\right]^{\beta_t}\right\}. \tag{28}$$

When explaining (28) in terms of t_F, the so-called probabilistic electro-thermal life model is derived, i.e., [6], [16], [54]

$$t_F(E', T') = [-\ln(1 - P_F)]^{1/\beta_t} \alpha_t(E', T') \tag{29}$$

which provides—at a given and constant value of failure probability P_F—the 100-P_Fth failure time percentile $t_F(E', T')$ of HVDC cable insulation subjected to stresses E' and T'.

Since $R(t_F) = 1 - P(t_F)$, where $R(t_F)$ is insulation reliability at mission time t_F [17], [50], from (29) the so-called reliability electro-thermal life model is attained, i.e.,

$$R(t_F, E, T) = \exp\left\{-\left[t_F/\alpha_t(E', T')\right]^{\beta_t}\right\}. \tag{30}$$

Hence, by definition the failure rate at time t_F, $h(t_F, E', T') = -[dR(t_F, E, T)/dt_F]/R(t_F, E', T')$, can be calculated by means of the following hazard function [17], [50]:

$$h(t_F, E', T') = \frac{\beta_t}{\alpha_t(E', T')}\left[\frac{t_F}{\alpha_t(E', T')}\right]^{\beta_t - 1}. \tag{31}$$

The practical way of using the probabilistic electro-thermal life model (29) to estimate the 100-P_Fth failure time percentile

$t_F(E', T')$, the reliability electro-thermal model (30) to estimate insulation reliability $R(t_F)$ at mission time t_F, and the hazard function (31) to estimate failure rate at mission time t_F—under the applied electrical and thermal stresses E' and T'—requires explaining $\alpha_t = \alpha_t(E', T')$ in (29)–(31) with a proper function of E' and T'. For HVDC cable insulation this can be done using one of the physical electro-thermal life models reported in Section III, or the phenomenological electro-thermal life model reported in Section IV: this latter either in the more general form (21) or in the form of the more popular IPM-Arrhenius electro-thermal life model (21), (22). For instance, by replacing $\alpha_t = \alpha_t(E', T')$ in (30) with the IPM-Arrhenius model (21), one gets the following IPM-Arrhenius reliability model at constant E and T:

$$R(t_F, E, T) = \exp\left\{-\left[\frac{t_F}{\alpha_0\left(\frac{E}{E_0}\right)^{-(n_0 - b_{ET}T')}\exp[-BT']}\right]^{\beta_t}\right\} \tag{32}$$

where α_0 is the value of α_t at $E = E_0$ and $T = T_0$.

An alternative, very interesting probabilistic framework for the IPM-Arrhenius electro-thermal life model is proposed in [65], where a piecewise power-law nonhomogeneous Poisson process and a stochastic electro-thermal model are proposed to predict total annual failures and failures due specifically to aging, respectively; an amalgamation of the two models is then used to estimate the number of failures attributable to random causes or aging. The proposed method is successfully applied in [65] to real data of vintage unjacketed XLPE 12 kV-ac cables; its application to HVDC cables would be very interesting, too.

VI. ENLARGEMENT OF HVDC CABLE INSULATION VOLUME

As pointed out in Section V, the insulation of HVDC cables is inherently nonhomogeneous and contains imperfections. Hence, the breakdown voltage of a small cable tested in the lab (mini-cable 1 of length l_1, inner insulation radius r_{i1}, and outer insulation radius r_{o1}) is greater than that of a power cable installed in the field (full-size cable 2 of length l_2, inner insulation radius r_{i2}, and outer insulation radius r_{o2}). From the Weibull hypothesis applied to the multiplication law for nondependent probabilities [50], the scale parameter of breakdown strength of the smaller-size mini-cable, α_{E1}, is related to the scale parameter of breakdown strength of the greater full-size cable, α_{E2}, by the following general relationship for HV cables [66], [67], [68], [69]:

$$\alpha_{E1}/\alpha_{E2} = G \times H = N_V \tag{33}$$

where G and H are functions detailed in Table II [16], [70].

1) G is the same for HVDC and HVAC cables, as it depends solely on geometrical parameters l_1, r_{i1}, l_2, r_{i2}, and on β_E.
2) H for HVDC cables is more complex than H for HVAC cables, as the latter depends only on r_{o1}, r_{o2}, β_E, while the former also on $\eta = (1 - \delta)\beta_E$, where $\delta =$ inversion coefficient of the dc electric field (see below) [68], [70].

TABLE II
FUNCTIONS G, H FOR HVAC AND HVDC CABLES [16]

Function	HVDC cables	HVAC cables
$G=$	$(l_2/l_1)^{1/\beta_E}$	$(r_{i2}/r_{i1})^{2/\beta_E}$
$H=$	$\left[\dfrac{2-\eta_1}{2-\eta_2}\dfrac{(r_{o2}/r_{i2})^{2-\eta_2}-1}{(r_{o1}/r_{i1})^{2-\eta_1}-1}\right]^{\frac{1}{\beta_E}}$	$\left[\dfrac{(r_{o2}/r_{i2})^{2-\beta_E}-1}{(r_{o1}/r_{i1})^{2-\beta_E}-1}\right]^{\frac{1}{\beta_E}}$

Functions G and H for HVAC cables were proposed for the first time in the milestone paper by Occhini [63], while function H for HVDC cables was developed in [68] and [69].

By merging the electro-thermal IPM-Arrhenius model (21) with the electro-thermal reliability model (32), and the statistical enlargement law (33), as detailed in [16] and [70], one attains the so-called enlarged electro-thermal reliability model

$$t_F(E, T)$$
$$= \alpha_0[-\ln(1-P_F)]^{1/\beta_t}\left(\frac{E}{E_0}\frac{N_V}{k_{P,E}}\right)^{-(n_0-b_{ET}T')}\exp(-BT') \tag{34}$$

$$k_{P,E} = \left[\ln(1-P_{E2})/\ln(1-P_{E1})\right]^{1/\beta_E} \tag{35}$$

where P_{E1} and P_{E2} are the breakdown probabilities of mini-cable 1 and full-size cable 2, respectively.

Equation (34) is complicated, but powerful, as it explains $t_F(E, T) = 100\text{-}P_F$th percentile of life of HVDC cable insulation in terms of electric field E, temperature T, cumulative failure probability P_F and insulation size [embedded in N_V, see (33)]. The name "enlarged electro-thermal reliability model" of (34) stems from the fact that it also serves to evaluate reliability and failure rate, as reliability $R = 1 - P_F$, and failure rate $h = -(dR/dt_F)/R$ [70].

In [49] and [56], the statistical enlargement law after [63] is refined for HVDC cables through the introduction of the dependence of breakdown strength on insulation thickness due to thermal instability. In this way, a general probabilistic life model similar to (34) is obtained [49], [56]

$$t_F = t_R\left[E/(E_2 H)\right]^{-n}\left[\log(1-P_D)/\log(1-P_t)\right]^{1/\beta_t} \tag{36}$$

where E_2 = reference maximum electric field for the full-size cable, with $t_R = t_F(E_2)$; P_D = design failure probability; P_t = test failure probability; $H = K_2/K_1$, with subscripts 1 and 2 referred to tested minicable and full-size cable, respectively, being $K = [(2\pi\lambda_{T,d}U_0^2\Delta T_d/W_d)/\log(r_o/r_i)]^{1/2}$, $\lambda_{T,d}$ = thermal conductivity of the dielectric, ΔT_d = temperature drop across the insulation, W_d = per unit length (p.u.l.) dielectric losses. This approach leads also to a VEC n tending to be higher at a higher electric field; this results in a shorter life at higher-than-design fields than that expected based on a constant n (as in Occhini's expression). This would be the case when evaluating the effects of over-voltages or high-field testing during qualification or ALTs [49].

In [40] and [41], the DMM life model described in Section III-B provided an alternative to infer the life of full-size cables from life expressions developed on thin laboratory specimens. In [40], the volume dependence of aging and life model parameters in the geometry of full-size cables was tackled through a "scaled-up" shell approach, based on the failure probability of multiple coaxial thin shells constituting the insulation—each with constant values of E and T, and scaled-up to the whole cable insulation volume. The methodology, applicable to any aging theory, can be used to infer cable lifetimes from thin film ALTs. Details are found in [40], but in summary, the results showed that in (4) for full-size cables the free energy barrier to aging was almost the same as for mini-cables, but the values of $A*$ and C' suggested that the larger cable contains centers more sensitive to the electric field and requiring less energy to trigger failure, as expected for a larger insulation volume.

In [41], extreme defects (e.g., large voids, stress-enhancing contaminants, etc.) were included in DMM model simulations to infer from thin specimens the time-to-failure of full-size cable insulation. The time-to-failure of broad XLPE samples was simulated on a 2-D 110×100 grid in plane-plane electrode arrangement; the 150 μm-spacings of the grid stand for the elementary parts of the broad sample, which are "broken" as an elementary bond (i.e., turned from insulating to conducting) as aging progresses. In [41], the aging of the broad sample was evaluated under constant stress in all elemental bonds via the DMM kinetic equations [in particular (5)] by assigning them randomly selected model parameter values from distributions obtained through ALTs on thin films. More details are omitted, but—broadening the simulations to cable arrangements—it was shown in [41] that lifetimes from high field ALTs should be regarded with great care, as they probe only the extreme most susceptible regions of the insulation, while cable life at service fields depends on a wider group of regions. The technique may help in cable insulation material choice, limiting the need for expensive ALTs on large-scale insulation systems [41].

A unified enlargement law of polymer breakdown strength under short pulses was given in [71]. It is skipped here as not directly relevant for HVDC cables—apart, maybe, voltage transients treated in Section VIII.

VII. LIFE ESTIMATION UNDER THERMAL TRANSIENTS

A. Procedure for Life and Reliability Estimation of HVDC Cables Subjected to Cycles of Load Current

The main thermal transients in the service life of HV cables are due to the periodic cycles of load current. A life and reliability estimation procedure for HVDC cables under load cycles was presented first in [54], and then improved in [55], [57], and [72]. The procedure—similar to that developed earlier for HVAC cables in [73], but much more complex to account for the peculiarities of dc cables—is split into six steps (see Fig. 3):

$$dLF(r, t) = \frac{dt}{L[E(r, t), T(r, t)]} \tag{37}$$

$$LF_{cycle}(r) = \int_0^{t_d} dt/L[E(r, t), T(r, t)] \tag{38}$$

$$K_{cycle}(r) = 1/LF_{cycle}(r) \tag{39}$$

$$L_{cycle}(r) = t_d \times K_{cycle}(r) \tag{40}$$

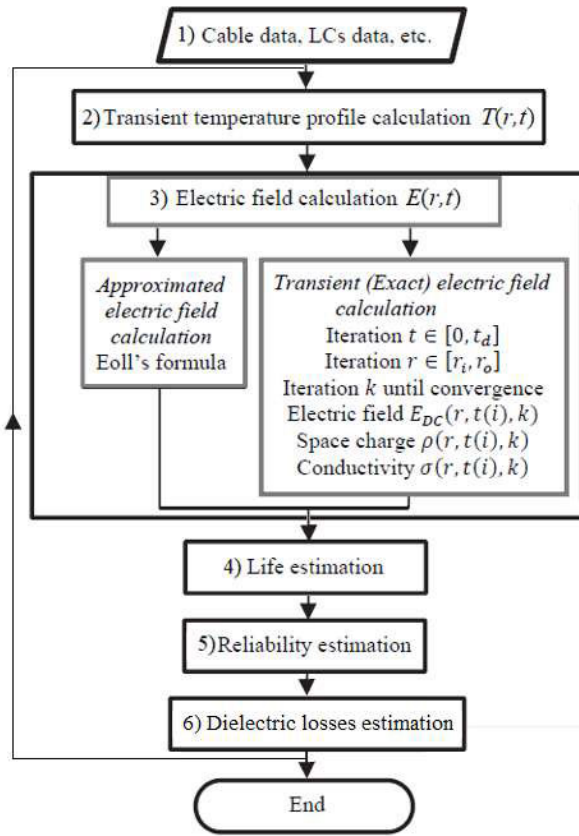$$L_{cycle}^* = \min\{L_{cycle}(r), r \in [r_i, r_o]\} = t_d \times K_{cycle}^*. \tag{41}$$

Fig. 3.   Flowchart of the procedure.

1) Cable and load cycle data are set. Daily cycles are taken, with a given function $I = f(t)$ describing the variation of load current I with time $t \in [0, t_d]$, where $t_d = 24$ h.
2) The transient temperature profiles $T(r, t)$ within cable insulation caused by load cycles are computed at each radial coordinate (or insulation radius) $r \in [r_i, r_o]$—being r_i and r_o respectively inner and outer insulation radii—and at each time $t \in [0, t_d]$ during the cycle. Computations follow IEC Standard 60853-2 [74], adapted to dc cables.
3) The field profiles $E(r, t)$ in cable insulation are computed from temperatures $T(r, t)$, either in an approximate way via the so-called Eoll's formula [75] (earlier procedure [54], left branch in block 3, Fig. 3), or in a rigorous way via Maxwell's equations (improved procedure [55], right branch in block 3), see Section VII-B.
4) The fractions of life $d\mathrm{LF}(r, t)$ lost by the insulation are calculated via (37) here below. $L[E(r, t), T(r, t)]$ in (37) is insulation life at $E(r, t)$ and $T(r, t)$, and can be derived with any physical or phenomenological electro-thermal life model valid for the insulation; in [54] and [55] the IPM-Arrhenius model in the form of (22) was used with theoretically and experimentally sound values of its parameters, as the IPM and the Arrhenius life models are, respectively, the reference electrical and thermal life models of International Standards for HVDC cable insulation (see Section IV-C). Thereafter, the fractions of life $LF_{\mathrm{cycle}}(r)$ lost during each cycle at each radius r are computed via (38) and, by setting to 1 the sum

of all $LF_{\mathrm{cycle}}(r)$ at failure (Miner's law of cumulated damage [76]), the number of cycles-to-failure , $K_{\mathrm{cycle}}(r)$, is determined via (39). Then, the life $L_{\mathrm{cycle}}(r)$ at each insulation radius r is derived via (40). Eventually HVDC cable life under load cycles, L^*_{cycle}, is evaluated via (41) as the life of the insulation at the most stressed radius r^*, i.e., the value of r yielding the minimum number of cycles-to-failure, K^*_{cycle}

$$\alpha^*_{t,cycle} = L^*_{cycle}/[-\ln(1 - P_D)]^{1/\beta_t}. \qquad (42)$$

5) The drop in cable insulation reliability over time due to load cycles is estimated to take life under load cycles, L^*_{cycle}, as a Weibull random variable distributed according to (25). In the IPM-Arrhenius model (22) employed in [54] and [55], the design cable life L_D at constant-stress corresponds to design failure probability P_D; thus L^*_{cycle} corresponds to P_D, too [54]. Hence, denoting with $\alpha^*_{t,\mathrm{cycle}}$ the 63.2th percentile of the life under load cycles [57], (25) can be recast for $P_F = P_D$, $t_F = L^*_{\mathrm{cycle}}$, $\alpha_t = \alpha^*_{t,\mathrm{cycle}}$ as [57]
Then, by inserting (42) for $\alpha^*_{t,\mathrm{cycle}}$ in (30) one can estimate the reliability at mission time t_F of HVDC cable insulation subjected to load cycles, as follows:

$$R(t_F) = \exp\{-(t_F/L^*_{cycle})^{\beta_t}[-\ln(1 - P_D)]\}. \qquad (43)$$

6) This step, added to the procedure in [72], serves to account for p.u.l. dielectric losses $W_d(t) = \int_{r_i}^{r_o} 2\pi r\sigma[E(r, t)]^2 dr$, to check their negligibility versus p.u.l. conductor losses $W_c(r, t)$, as is mostly the case in qualified cables [77]. If this holds the procedure is ended; otherwise temperature profiles $T(r, t)$ are updated and all calculations are repeated until convergence, to rule/single out thermal runaway.

A key comment to this procedure is that insulation life under load cycles L^*_{cycle} is the minimum value of life $L_{cycle}(r)$ over insulation thickness at the critical radius $r^* \in [r_i, r_o]$ of maximum stress. Finding r^* is trivial in HVAC cables, as the maximum values of E and T always lie at the inner semicon/insulation interface; it is not in HVDC cables, where the most stressed point varies with the load. This is due to the dependence of the electric field in dc cables on electrical conductivity σ, which in turn depends on the field and especially on temperature, as shown by the following empirical formula by Klein [78] (other relationships $\sigma = f(E, T)$ can be found e.g., in [6, Ch. 3] and [79]):

$$\sigma = \sigma_0 \exp[a(T - T_0) + b(E - E_0)] \qquad (44)$$

where σ_0 is the value of σ at reference electric field E_0 and temperature T_0, a and b are the temperature and stress (or field) coefficients of electrical conductivity.

Therefore, the calculation of the electric field in dc cables is critical in the above procedure and deserves more details.

B. Field Calculation in HVDC Cables Under Load Cycles

As hinted at above, in the earlier version of the procedure for life and reliability estimation of HVDC cables subjected to load cycles [54] the electric field in HVDC cables was

computed in an approximate way [75], while in the improved version [55] it is computed rigorously via Maxwell's equations [6], [80].

The approximated calculation of electric field in dc cables stems from the following equation, holding in steady-state [80]:

$$E(r) = U_{dc} \frac{r^{z-1} \exp[-bE(r)]}{\int_{r_i}^{r_o} r'^{z-1} \exp[-bE(r')]dr'} \tag{45}$$

where U_{dc} = applied dc voltage; $z = a\Delta T_d/ln(r_o/r_i)$; $\Delta T_d = T(r_i) - T(r_o)$ = temperature drop across cable insulation. Equation (45) neglects the transient electric field that occurs between the quasi-capacitive field distribution found right after U_{dc} is applied across cable insulation and the purely resistive field is achieved at a steady state when (45) holds.

In addition, as described in [6] and [75], the approximated method skips the iterative numerical solution of the transcendent relationship (45) by recasting it into the following simplified "Eoll's formula," named after its first proposer:

$$E(r) = U_0 \frac{\delta}{r_o[1 - (r_i/r_o)^\delta]} (r/r_o)^{\delta-1} \tag{46}$$

$$\delta = \frac{\frac{aW_c}{2\pi\lambda_{T,d}} + bE_m}{1 + bE_m} = \frac{\frac{a\Delta T_d}{\ln(r_o/r_i)} + \frac{bU_0}{r_o-r_i}}{1 + bU_0/(r_o - r_i)} \tag{47}$$

where E_m is the mean value of the electric field; W_c are p.u.l. conductor losses; $\lambda_{T,d}$ is the thermal conductivity of the dielectric; δ is the "field inversion coefficient," such that field inversion (i.e., the displacement of a maximum electric field from inner to outer insulation as the load rises) occurs whenever $\delta > 1$ [6].

According to the more rigorous approach to transient field calculation in dc cables [80]—introduced in the procedure in [55]—the transient electric field under dc voltage is calculated numerically in an iterative way using Klein's conductivity expression (44) plus time-dependent Maxwell's Equations with permittivity ε taken as constant over time, i.e., [6], [79], [80], [81]

$$\text{Gauss law} \quad \rho - \nabla \cdot (\varepsilon \boldsymbol{E}) = 0 \tag{48}$$

$$\text{Current continuity} \quad \partial\rho/\partial t + \nabla \cdot \sigma \boldsymbol{E} = 0 \tag{49}$$

where E = electric field vector, ρ = free charge density, $\sigma E = J$ (Ohm's law), J = conduction current density vector.

C. Illustrative Applications of the Procedure

In principle, the procedure for life and reliability estimation of HVDC cables subjected to load cycles can be applied to whatever pattern of load cycles, but in [54], [55], and [57] 24-h (daily) and 48-h load cycles only were considered. This is not solely for the sake of simplicity, but also as daily load cycles well describe the service of HV cable systems; in addition, 24-h and 48-h load cycles of different types are applied during the qualification tests of HVDC cables according to [9] and [10].

The earlier procedure (based on the approximate field from Eoll's formula [54]) and the improved procedure (based on the rigorous field from Maxwell's equations [55]) were employed in [54], [55], and [57] to evaluate the PQT life and the TT

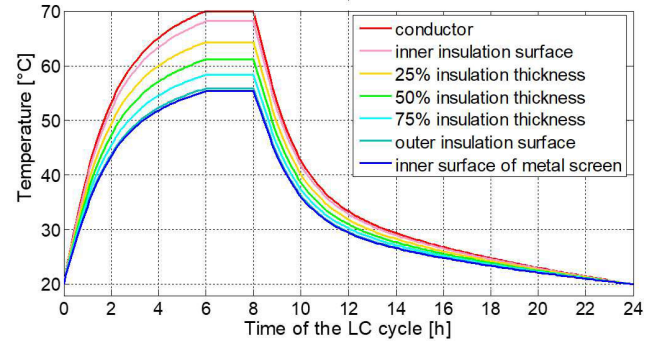| Parameter	Value
Rated DC voltage / power / converter	320 kV /1105 MW / VSC
Conductor material /Rated temperature /X-section	Cu / 70°C / 1600 mm²
Insulation material / thickness	DC-XLPE /17.9 mm
Design life L_D / fail.robability P_D / reliability R_D	40 years / 1 %/ 99%
Laying environment type / temperature	Soil / 20 °C

Fig. 4. Transient temperatures in a load cycle of the LC period [9] at seven insulation radii of the studied cable. After [55].

life—i.e., the life under the load cycles prescribed in [9] for the PQT and the TT, respectively, of HVDC extruded cable systems—of a 320 kV-dc XLPE-insulated land cable used with voltage source converters (VSC). Let us start with PQT life evaluation in [55] through steps 1)–4) of the procedure (see Fig. 3) as PQT is vital for long-term cable reliability.

Starting from step 1, the main design parameters of the studied cable are quoted in Table III. As for the load cycles, the PQT for VSC cables consists of 360 "24-h" cycles at dc voltage $U_{PQT} = 1.45U_0$, grouped in three periods, i.e., "true" load cycles (LC period), high load (HL) period, and zero load (ZL) period [9]. Step 1 was completed in [55] by setting also: the parameters of CIGRÉ transient thermal network to the values from [74], [82]; the conductivity parameters in (44) to the values listed in Table IV—the low set (a_L, b_L), the medium set (a_M, b_M) and the high set (a_H, b_H) of coefficients a and b are taken from [79] to perform a sensitivity analysis of the field to typical ranges of a, b for dc-XLPE; the values of parameters in life model (22) to the same values chosen in [54], i.e., $L_D = 40$ y, $P_D = 1\%$ ($R_D = 99\%$), $n_D = 10$ [7], [9], [56], $B = 12\,430$ K, $b_{ET} = 0$.

Moving on to step 2 of the procedure, Fig. 4 after [55] shows the transient temperature profiles $T(r, t)$ during the 24-h load cycles of the LC period at 7 radii within the insulation of the studied cable; these profiles agree with the prescriptions in [9].

Coming to step 3, Fig. 5 after [55] shows the transient electric field profiles $E(r, t)$, calculated with the rigorous method during one load cycle of the LC period at 5 radii in the insulation of the studied cable for a_L, b_L. These profiles hold from the third cycle on, as then transient field profiles become stable within each cycle. Detailed comments on Fig. 5 appear in [55].

Passing to step 4, Table V after [55] quotes insulation life $L_{cycle}(r)$ obtained from (37) to (41) with $E(r, t)$ calculated for a_L, b_L, a_M, b_M, and a_H, b_H via the rigorous and approximate method, at inner, mid (50% thickness) and outer insulation of
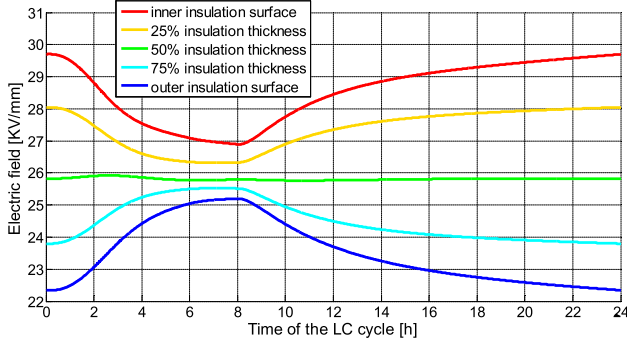
Fig. 5. Transient electric field profiles during one daily load cycle of LC period at 5 radii in the insulation of the studied cable computed with the rigorous method for a_L, b_L. After [55].

TABLE IV
VALUES OF CONDUCTIVITY PARAMETERS AFTER [79]

	σ_0 [S/m]	a [1/°C]	b [mm/kV]
Low set (a_L,b_L)	10^{-16}	0.042	0.032
Medium set (a_M,b_M)	10^{-16}	0.084	0.0645
High set (a_H,b_H)	10^{-16}	0.101	0.0775

TABLE V
INSULATION LIFE $L_{\text{CYCLE}}(r)$ WITH RIGOROUS AND APPROXIMATE FIELD PROFILES FOR a_L, b_L, a_M, b_M, AND a_H, b_H, AT INNER, MID, AND OUTER INSULATION OF THE STUDIED CABLE. PQT LIFE L_{CYCLE}^* IS DENOTED BY A GRAY-SHADED CELL. AFTER [55]

	$L_{cycle}(r)$ [y]					
a,b values→	a_L,b_L		a_M,b_M		a_H,b_H	
insul. radius ↓	exact field	approx. field	exact field	approx. field	exact field	approx. field
inner, r_i	2.32	2.93	4.19	5.32	7.29	9.22
mid, $0.5(r_o-r_i)$	7.32	7.17	4.44	4.39	5.86	5.83
outer, r_o	17.8	14.4	4.35	3.77	4.64	4.05

the studied cable. The values of PQT life L_{cycle}^* (gray-shaded cells) derived with the rigorous and the approximate field are fairly different; moreover, for a_M, b_M the rigorous field locates L_{cycle}^* at inner insulation ($r^* = r_i$), whereas the approximate field at outer insulation ($r^* = r_o$). Details of the explanation are found in [55].

Dealing with step 5 of the procedure (reliability estimation, see Fig. 3), this step is skipped in [54] and [55]; on the contrary, in [57] an application of the life and reliability procedure for the studied cable of Table III subjected to TT load cycles after [9] is reported that includes reliability calculations. The electrical TT for HVDC VSC extruded cables consists of a first series of 24 24-h load cycles plus a second series of three 48-h load cycles, all under a dc voltage $U_T = 1.85U_0$, for a total duration of 30 days. For brevity, let us omit here the results of steps 1)–4) and report from [57] only Fig. 6, where (for a_M, b_M) the reliability of the studied cable under TT load cycles at $U_{\text{TT}} = 1.85U_0$, evaluated via (43), is compared to that evaluated via (32) at U_{TT} with conductor temperature set to 70 °C (= design temperature), i.e., skipping the effect of thermal stress and electro-thermal synergism on insulation life and reliability during TT load cycles; this latter is the way of [9] for estimating TT duration = TT life from (14). In Fig. 6,the reliability curve from (32) (dashed line), which neglects the thermal effects of load cycles, reaches design reliability $R_D = 0.99$ after 30 days, in line with [9]; the reliability curve from (43) (solid line), which considers
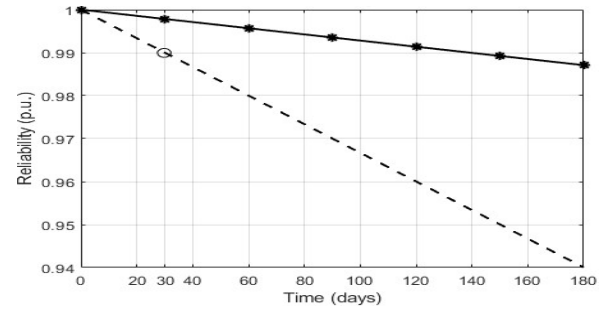

Fig. 6. Reliability of the studied cable versus aging time at $U_{\text{TT}} = 1.85U_0$ with TT load cycles [(43), solid line] and without TT load cycles [(32), dashed line]. a_M, b_M. After [57].

the thermal effects of load cycles, lies well above the former curve and reaches $R_D = 0.99$ after ≈ 140 days, since when such effects are considered [57], mean conductor temperature is <70 °C (see Fig. 4), and cable life is longer than the TT duration.

Closing with step 6 (dielectric losses estimation), in [72] the p.u.l. dielectric losses W_d for the studied cable at 70 °C and voltages U_0, $U_{\text{PQT}} = 1.45U_0$, $U_{\text{TT}} = 1.85U_0$ are 0.06, 0.2, 0.6 W/m, respectively. Being more than negligible versus p.u.l. conductor losses W_c at 70 °C, i.e., 40 W/m, the procedure can be ended.

Overall, these applications yield much longer PQT and TT lives than the duration, respectively, of the PQT (=360 days ≈ 1 year) and the TT (30 days). This indicates that the PQT and TT with maximum conductor temperature set exactly to design temperature T_D might not be challenging enough [54], [55], [57].

VIII. LIFE ESTIMATION UNDER VOLTAGE TRANSIENTS

It is also crucial to estimate how the various transient voltage waveforms found on duty affect the life and reliability of HVDC cables [2]. While many simulations were done over the years for the evaluation of transient voltages like lightning overvoltages, switching overvoltages, and TOVs in HVDC cables (see [83], [84], [85], [86], [87]), few life and reliability models were developed for HVDC cables subjected to transient voltages. This section reviews these models focusing for brevity on long TOVs, SSIs, and VPRs.

A. TOVs and SSIs

Many simulations (see e.g., [84], [85], [86]) proved that in HVDC cables with VSC in modular multilevel converter (MMC) arrangement, long TOVs take place on one pole in case of a pole-to-ground fault on the other pole, or of a phase-to-ground fault on the ac side of the converter. As these long TOVs might affect cable system reliability, CIGRÉ Joint Working Group (JWG) B4/B1/C4.73 has analyzed the issue of the surge and extended over-voltage testing for MMC HVDC cable lines in monopolar and rigid bipolar schemes [87]; the most critical long TOV was found to be due to a pole-to-ground fault in a symmetric monopolar VSC MMC HVDC cable line, yielding a top overvoltage of ≈ 1.8 p.u. of rated dc voltage U_0 amid the healthy pole [84], [85] (see Fig. 7 after [88]).
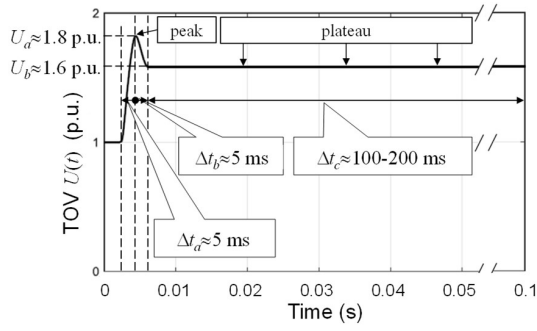
Fig. 7. Worst case long TOV $U(t)$, in p.u. of rated dc voltage U_0, in a symmetric monopolar VSC HVDC cable line. After [88].
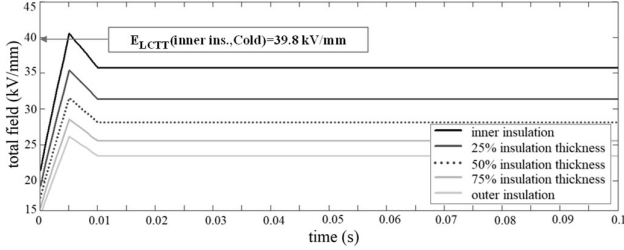

Fig. 8. Electric field during the TOV of Fig. 7 in the insulation of the studied cable in cold conditions with a_L, b_L. After [89].

In [89], this "worst case" TOV was tackled to evaluate the severity of long TOVs for HVDC cables, by computing the following:

1) The electric field in the insulation during such TOV.
2) The life fraction lost during one single worst-case TOV.

The total electric field, $E_{TOV}(r, t)$, during the worst case TOV $U(t)$ of Fig. 7 was obtained versus cable insulation radius r and time $t \in [0; \Delta t_{TOV} = \Delta t_a + \Delta t_b + \Delta t_c]$ as the sum of [6], [80], [89].

$$E_{TOV}(r, t) = E_{dc,U0}(r) + E_{ac}(r, t). \quad (50)$$

1) $E_{dc,U0}(r)$, the resistive steady-state dc field due to U_0;
2) $E_{ac}(r, t)$, the capacitive "ac-like" field due to the transient component $U(t)–U_0$ of the long TOV

$E_{dc,U0}(r)$ was calculated via steady-state Eoll's formula (46), with the sets of conductivity coefficients a_L, b_L, a_M, b_M, a_H, b_H shown in Table IV [75], [77]. Indeed, the TOV of Fig. 7 cannot alter the steady-state dc field set by U_0, since time intervals Δt_a, Δt_b, Δt_c ($\Delta t_a \approx \Delta t_b \ll \Delta t_c$) are overwhelmed by time 10τ to steady state field in polymers for HVDC cables [7], [9] (being $\tau = \varepsilon/\sigma$ the dielectric time constant), both when the cable is hot, i.e., at full load, and a fortiori when it is cold, i.e., without load.

$E_{ac}(r)$ was calculated as follows [80]:

$$E_{ac}(r, t) = [U(t) - U_0]/[r \ln(r_o/r_i)]. \quad (51)$$

In this way, for the studied cable of Table III the maximum of $E_{TOV}(r, t)$ was found at inner insulation for both cold and hot cable conditions, with the absolute maximum observed for the cold cable with a_L, b_L (see Fig. 8 after [89]).

Coming to the life fraction $\Delta LF(r^*)$ lost during one worst-case TOV of duration Δt_{TOV} at the point of highest electro-thermal stress in the insulation, $r^* = r_i$, in [89] it was estimated similar to step 4 of the life estimation procedure

TABLE VI
LOSS-OF-LIFE FRACTIONS AT INNER INSULATION IN COLD AND HOT CABLE CONDITIONS WITH a_L, b_L, a_M, b_M, a_H, b_H: WORST CASE TOV VERSUS SSISP. AFTER [91]

a,b set ↓	waveshape ↓	Cold Cable		Hot Cable	
		loss-of-life fra.	Δ(%)	loss-of-life fra.	Δ(%)
a_L,b_L	SSISP	4.5×10^{-8}	-	2.2×10^{-8}	-
	TOV(Δt_c=100 ms)	1.0×10^{-7}	+122	3.7×10^{-8}	+68.2
a_M,b_M	SSISP	1.2×10^{-8}	-	4.5×10^{-9}	-
	TOV(Δt_c=100 ms)	2.6×10^{-8}	+117	6.0×10^{-9}	+33.3
a_H,b_H	SSISP	8.8×10^{-9}	-	3.0×10^{-9}	-
	TOV(Δt_c=100 ms)	1.8×10^{-8}	+105	3.8×10^{-9}	+26.7

of HVDC cables under load cycles, i.e., (see (37),(38) at Section VII-A)

$$\Delta LF(r^*) = \int_{\Delta t_{TOV}} dLF(r^*, t) = \int_{\Delta t_{TOV}} \frac{dt}{L[E^*_{TOV}, T^*_{TOV}]} \quad (52)$$

where $L[E^*_{TOV}, T^*_{TOV}]$ is insulation life in the field $E^*_{TOV} = E_{TOV}(r_i, t)$ and temperature $T^*_{TOV} = T(r_i, t) = T(r_i)$. T^*_{TOV} is $\approx$ constant over a very short time (from a thermal viewpoint [90]) $\Delta t_{TOV} \approx 100$ ms, thus $L[E^*_{TOV}, T^*_{TOV}]$ can be computed from the sole variation of the field E^*_{TOV} over Δt_{TOV} via any physical or phenomenological electrical life model valid for the insulation; in [89] the IPM of (14) was used with $n_0 = 10$, $L_0 = 40$ years, $E = E^*_{TOV}$, $E_0 = $ design field of insulation at $r = r_i$, since the IPM with $n_0 = 10$, $L_0 = 40$ years is the reference electrical life model of International Standards for HVDC extruded cable insulation [7], [9] (see Table I).

The same approach was used in [91] to evaluate the severity of SSIs applied during TTs after [7], [9] and compare them with the worst-case TOV in terms of the fraction of life lost in one single surge. Both SSI of the opposite polarity (SSIOP) to rated dc voltage U_0 and SSI of the same polarity (SSISP) as U_0 were analyzed, always finding the maximum field at inner insulation in both cold and hot cable conditions (with the absolute maximum for cold cable and a_L, b_L), as for the TOV [91]. Table VI after [91] reports the loss-of-life fractions at inner insulation in cold and hot cable conditions obtained with a_L, b_L, a_M, b_M, and a_H, b_H for the SSISP (providing a higher maximum field than the SSIOP) versus those for the worst case TOV. For both the TOV and the SSISP [89], [91]: the life fractions lost at inner insulation are higher for the cold than for the hot cable, since in both cases the field is higher for the cold than for the hot cable; the loss of life at inner insulation drops as a, b increase, since in both cases the maximum field at inner insulation also drops as a, b increase. The percent difference Δ between the loss-of-life estimates for TOV and SSISP highlights that the worst-case TOV has always higher loss-of-life fractions than the SSISP, mainly due to the long plateau of the TOV of Fig. 7. Anyway, the loss-of-life estimated for the worst case TOV—included the most critical case, i.e., inner insulation, cold cable, a_L, b_L—is very low. Thus, since the failure event leading to such TOV is very rare according to the typical failure rate of HVDC cables [58], the overall loss-of-life cumulated by the cable in

service due to worst-case TOVs should be negligible and not of main concern.

However, these results should be taken with care due to the approximations on which the loss-of-life fraction estimates rely [89], [91], first and foremost, the use of the IPM with a given value of n_0 at both design field and maximum field during the TOV and SSISP. For this reason, to target a conservative upper limit of the aging effects of long TOVs, in [88], the procedure for estimating the loss-of-life fractions during the worst-case TOV was improved accounting for the following:

1) The effects of cable line length on insulation volume, via the enlarged reliability model for HVDC cables (34).
2) The peculiar challenge added by the very fast peak of the TOV of Fig. 7 (lasting $\Delta t_a + \Delta t_b \approx 10$ ms) to that of the much longer plateau (lasting $\Delta t_c \approx 100$ ms), via a life model for insulation affected by voltage harmonics [92], [93].

In this way, relationship (52) was recast as follows [88]:

$$\Delta\mathrm{LF}(r^*) = \left(\frac{l_2}{l_1}\right)^{\frac{n_0}{\beta_E}} \left\{ \int_{\Delta t_a + \Delta t_b} \frac{dt_{\mathrm{peak}}}{L_{\mathrm{pla}}\left(K_{p,\mathrm{TOV}}\right)^{-n_{p,\mathrm{TOV}}}} \right.$$
$$\left. + \int_{\Delta t_c} \frac{dt_{\mathrm{plateau}}}{L_0\left(E^*_{\mathrm{TOV}}/E_0\right)^{-n_0}} \right\} \quad (53)$$

where $L_{\mathrm{pla}} = L_0[E_{\mathrm{pla}}/E_0]^{-n_0}$; $E_{\mathrm{pla}} =$ plateau field of TOV at $r^* = r_i$ computed from (51) with $U(t) = U_b = 1.6U_0$ (see Fig. 7); $K_{p,\mathrm{TOV}} = E_{p,\mathrm{TOV}}/E_{\mathrm{pla}}$, $E_{p,\mathrm{TOV}} =$ peak field of TOV at $r^* = r_i$, derived from (51) with $U(t) = U_a = 1.8U_0$; $n_{p,\mathrm{TOV}} =$ exponent accounting for the aging effects of the peak of ac + dc field, set to 15 after [92], [93].

In [88], for long lines and conservative values of insulation parameters, the improved procedure provides three orders of magnitude higher loss-of-life fractions than those in Table VI; such higher loss-of-life fractions might be nonnegligible for severely-aged cables in service for a long time.

Experimental studies were carried out to assess the aging effects of TOVs and SSIs on HVDC cable insulation [94], [95], [96], but they did not provide direct outcomes for life and reliability models so far. XLPE samples subjected to a large number of TOVs in [94] and of SSIs in [95] showed a mild increase of complex permittivity ε," perhaps due to dipolar polarization; indeed FT-IR tests showed that C=O and C–O bonds—typical of oxidation—appear on aged sample surface: a sign of aging, as the greater the amplitude and the number of applied TOVs and SSIs, the greater these effects. In [96], a sound and broad test campaign focused on the pulsed electro-acoustic (PEA) cell, studied the space charge behavior of XLPE under SSIs.

B. Voltage Polarity Reversals

Nowadays the service of HVDC cable systems is more dynamic, being linked to the electricity market, which requests an increasing number of power flow inversions. Power flow is inverted via current direction reversal (CDR) in VSCs, via VPR in line commutated converters (LCCs). VPRs are of two different types [97] as follows:

1) Slow VPRs, where dc voltage goes from $+/-U_0$ to 0 in ≈ 0.5 s, stays to 0 over a relaxation period of a few minutes, and eventually goes to $-/+U_0$ in ≈ 0.5 s.
2) Fast VPRs, where no relaxation period exists.

While CDRs set no challenge to HVDC cables, VPRs are critical especially for HVDC extruded cables due to space charge storage under dc voltage in polymeric insulation [1], [2], [6], [18], [98]. Thus, so far lapped cables—particularly of the MIND type—are the only HVDC cable type used with LCCs, except the 2012 Honshu-Hokkaido link in Japan [6]. Anyway, also MIND cables need to be rescued from excessive VPRs, hence manufacturers limit the number of yearly VPRs and set a minimum rest interval between two adjacent VPRs [97]. Thus, it is crucial to develop life and reliability models also for HVDC LCC cables subjected to fast and slow VPRs.

An early trial led to a phenomenological-physical life model for HVDC polymeric cables under fast VPRs, namely [99]

$$L_{Ni}/L_i = 1 + K E^{b_1} f'^{A_5"} \quad (54)$$

where L_{Ni} and L_i are the values of life at field E without and with VPRs; $f' = f/f_0$, f being VPR frequency and f_0 a reference VPR frequency; K, b_1, A_5" are physical-phenomenological quantities attained via life tests and space charge measurements.

A similar model was proposed in [100] to reproduce the results of load cycle tests with fast VPRs performed on full-size HVDC MIND cables on behalf of Terna (the Italian TSO); here the key was computing the field during the VPR transient via a complex heuristic method based on space charge relaxation. Another model was proposed in [97] to estimate the life of HVDC MIND cables under load cycles plus slow VPRs, based on the procedure for load cycles described in Section VII-A plus manufacturers' experience for evaluating the relaxation time constant of space charges—and the related variation of the field in the insulation—during and after a slow VPR. In this way, life values matching Terna's experience with load cycle tests with VPRs on HVDC MIND cables were attained.

A more general model is being developed by the same authors at present, where the calculation of the electric field during and after fast and slow VPRs is done using the rigorous method for transient electric field based on Maxwell's equations [80] described in Section VII-B. The relevant field calculations appear in [101], but they have not been integrated into a life model yet. It should be noted that calculations of transient fields in HVDC cables have been performed—even in the complex geometry of joints—by developing their own codes [102] or using commercially available software (e.g., Comsol Multiphysics) [103], [104], but even such calculations have not been integrated into a life model yet.

The effect of different ambient temperatures and load currents, along with VPRs and load cycles on the distribution of electric field and temperature in the insulation of an HVDC XLPE cable is analyzed in [105], but without using these calculations in any life and/or reliability model.

C. Gaps in the Life and Reliability Estimation of HVDC Cables Subjected to Thermal and Voltage Transients

Maybe the main gap in the literature on life and reliability estimation of HVDC cables subjected to thermal and voltage transients is that—as to the author's best knowledge—the physical models presented in Section III were never applied in the literature so far for life estimation under thermal transients (this is also why physical models are missing in Section VII-C), as well as under voltage transients (this is also why physical models are missing in the present Section VIII). It should be pointed out that—again, as to the author's best knowledge—all treatments relevant to life estimation of HVDC cable insulation under thermal transients so far are relevant to the thermal transients associated with qualification load cycles according to CIGRE TB 496:2012 [7] and CIGRE TB 852:2021 [9]: in these TBs, the IPM in the form of (14) is taken as the reference life model for setting voltage levels and durations of load cycle tests (see Table I). For this reason, although any physical or phenomenological electro-thermal life model valid for the insulation could be used in the procedure for HVDC cable life estimation under load cycles, only the IPM-Arrhenius model—that merges the IPM electrical model with the Arrhenius thermal model, this latter being the basis of IEC std. 60 216 for thermal aging of insulation—is used in such a procedure applied to qualification load cycles [54], [55], [57].

Moreover, the usage of physical life models (1)–(11) for full-size HVDC cables is much more cumbersome than that of the following:

1) The IPM-Arrhenius model (22) used in Section VII-C for load cycles and Section VIII-B for load cycles plus VPRs.
2) The IPM (14) used in Section VIII-A for long TOVs and SSIs.

This is quite evident when comparing (1)–(11) with (14) or (22), considering also that in (14) and (22) a direct reference can be made to the design life and voltage of the full-size cable, which is not possible in (1)–(11).

However, the missing use of physical life models for life estimation under thermal and voltage transients is a gap in the literature. Thus, the author's research team is committed to using physical life models for future estimations of the life and reliability of HVDC cable insulation under thermal and voltage transients, also as a useful contribution to the NEWGEN project.

IX. DISCUSSION

The various life and reliability models for HVDC cables illustrated in Sections III–VIII for different operating conditions (steady-state, load cycles, TOVs, SSIs, and VPRs) have of course some limitations, as they rely on simplifying hypotheses. A first simplifying hypothesis of phenomenological life models shown in Section IV and employed in Sections VII and VIII is that they use the same constant parameter values throughout service life without updating them to follow cable insulation degradation, while most physical life models shown in Section III stem from aging models and follow the degradation process, identifying the onset of failure as soon as some aging-related quantity reaches a critical value [27], [29], [31], [34], [43]. As an example, the procedure for life and reliability estimation of HVDC cables under load cycles described in Section VII uses the phenomenological IPM-Arrhenius model (22) with constant values of parameters n_0, B, b_{ET}, as well as of conductivity parameters σ_0, a, and b in (44) all over cable life. However, let us note that phenomenological parameters n_0, B, b_{ET} do not come from aging tests, but from ALTs carried out until failure; thus it is reasonable that they are kept unchanged all over insulation life. As for conductivity parameters σ_0, a, and b, it is expected that electrical conductivity is sensitive to insulation aging; however, in the extensive, long-lasting aging and ALT campaign on dc-XLPE specimens reported in [60] the electrical conductivity of specimens aged for a long time under different combinations of field and temperature did not show remarkable changes versus aging time. This suggests that the main changes in conductivity occur close to failure when the severely degraded insulation turns quickly from insulating to conducting; this happens also to other diagnostic properties of electrical insulation, such as breakdown strength and tensile strength [14], [51]. There is also a theoretical justification of this situation, made using the physical model of [41], which shows that material degradation that would result in changes in dielectric properties—such as conductivity—is very small for a very large percentage of the insulation life, as described in [106]. Thus, this first simplification does not seem critical.

Another simplifying hypothesis of phenomenological life models in Sections IV, VII, and VIII is that they take cable insulation implicitly as homogeneous, with two main consequences.

First of all, field calculation in dc cables, through both the approximated and the rigorous conductivity-based methods shown in Section VII-B, leads to a delocalized space charge distribution, continuously varying with position according to the ratio permittivity/conductivity $\varepsilon/\sigma = \tau$ (dielectric time constant) [80], [107]. If the constant ε hypothesis holds, this space charge distribution is due only to the spatial variation of σ caused by field and temperature gradients in cable insulation. However, this approach cannot predict the local space charge—both at electrodes and in insulation bulk—revealed by a big deal of measurements, see e.g., [6], [108], [109]. In fact, HVDC cable insulation is nonuniform, with contaminants and defects in its macro/microstructure [18], [110] leading to local space charge accumulation (see Section III-B). Local space charge effects on electric fields are important [47], [111], and their consideration requires a study of charge carrier injection and transport within the dielectric. Many studies (see e.g., [110]) over the years led to a 1-D bipolar charge transport model based on Maxwell's equations for computing charge density and field in PE in steady state [112], [113], including four charge carriers (mobile electrons and holes, trapped electrons and holes), with detrapping and recombination. This bipolar charge transport model was broadened to the cylindrical cable geometry under a time-constant temperature gradient in [114], and under a time-varying temperature gradient in [115] and [116]; eventually, the conductivity-based model (44), (48), (49) and the bipolar charge transport model were compared in [117], showing that the field results of

the bipolar charge transport model fit better the experimental observations.

Such effects of local space charge were skipped so far in the procedure for life and reliability estimation of HVDC cables under load cycles described in Section VII [54], [55], [57], as well as in the procedures for life and reliability estimation under-voltage transients treated in Section VIII [88], [89], [91], [97], [100], [101]. However, these procedures provide an overall picture of the life and reliability performance under thermal and voltage transients of state-of-the-art well-designed newly-manufactured full-size HVDC cables—i.e., those that are being currently manufactured, qualified after CIGRE TBs 496/852/ 853 and installed worldwide. Indeed, as pointed out in [47] and [118], experience shows that in such cables local space charge effects should not be a major concern either at rated fields or at qualification test fields. In fact, the voltage levels and durations of prequalification and TTs are derived in CIGRE TBs 496/852/853 taking the insulation as homogeneous and free of local charge: this is witnessed by the use of the IPM in the form of (14), where design and test voltage across the whole insulation thickness appear (see Table I), irrespective of possible inhomogeneities and local charge distributions within the insulation. However, a tool is now available for checking the significance of local space charge effects on qualified cables: it is IEEE std. 1732-2017 [119], which recommends a procedure for space charge measurements in full-size HVDC extruded cables before and after qualification tests. In HVDC cables qualified after CIGRE TB 496/852/853, local space charge effects should not be a major concern even at the long TOV fields, unless these latter fields trigger particularly-dynamic phenomena, like fast charge packets, as discussed extensively in [91].

Anyway, the author's research team is currently engaged in setting up a bipolar charge transport model for field calculation—for which the excellent studies done in papers [112], [113], [114], [115], [116], [117] are taken as a reference—to be added to the procedure for life estimation under load cycles (as well as, subsequently, to the procedure for life estimation under-voltage transients). In this way, the procedure will become capable of calculating local space charge density closer to reality, so as to account for the effect of charge density and its variation in the bulk.

A second consequence of the homogeneous insulation hypothesis is that even the unavoidable local inhomogeneities and defects, emphasized in physical models, are uniformly spread in the insulation, and the most severely stressed point in the insulation fails first, irrespective of its real microstructure. Actually, defects are not uniformly spread in HVDC cable insulation, both of the extruded and a-fortiori of the lapped type. Nonuniform defects should not have significant effects on the above-mentioned well-designed cables that pass qualification tests according to International Standards [118], but this might not hold for defective and/or more or less severely aged cables, particularly when voltage and load vary with time [120]. If strong nonuniformities take place in cable insulation, the most stressed point might not fail first if it is stronger enough than other less-stressed but weaker points [40], [41]. Strong nonuniformities will also

affect the steady-state and transient field distributions; then, the "traditional" evaluation of electric field in dc cables according to [80]—illustrated in Section VII-B as a fundamental step for life and reliability estimation under thermal transients (see Section VII) and voltage transients (see Section VIII)—might not be fully adequate, and more sophisticated calculation methods are advisable, as those in [81], [120], and [121].

In [120], approximate exponential expressions—based on electrical and thermal time constants of polymeric dielectrics—are proposed for transient electric field inside a cavity in an HVDC extruded cable during voltage and thermal transients like energization, VPRs at rated load, load cycles at rated voltage; they serve to evaluate the PD inception field, the repetition rate and the inception voltage at steady state and during transients. The results in [120] show that in defective HVDC extruded cables under transients, the PD repetition rate may be as large as under ac voltage, thus causing significant aging even if transients last only minutes or hours. This is often not properly accounted for at the design stage, even if the insulation is designed to bear the rated steady-state electro-thermal stress without PDs throughout cable life.

Developing this approach, in [121], PD charge amplitude and repetition rate are studied in a cavity within dc cable insulation under a transient voltage as a function of voltage slew rate, evaluating the cumulative extent of aging associated with PDs at different slew rates. The theoretical model in [121] fits well measurements on multilayer specimens of a PP compound for HVDC cables with a cylindrical cavity, tested via two different voltage slew rates, i.e., 0.05 and 1 kV/s, up to a steady value of 20 kV—above the PD inception voltage (PDIV) in dc and ac. Results in [121] show that a reduction of voltage slew rate, electrical conductivity, and conductivity dependence on temperature and field reduces dc cable insulation damage due PDs during voltage transients like energization or VPRs.

A further simplifying hypothesis of the "traditional" method for dc cable field calculation [80] shown in Section VII-B is that it considers only the nonlinear, steady-state dependence of electrical conductivity on T and E via e.g., (44), neglecting the time/frequency dependence of permittivity ε associated with dipolar and interfacial polarization which affects the field transient duration, thus cumulated aging. This assumption may be good for the "only-slightly-polar" polymeric insulation of extruded cables, but it may be not e.g., for the multilayered rubber insulation of accessories with multiple interfaces [122]. In [81], the traditional method for field calculation in dc cables is broadened considering time-varying dielectric polarization through Debye's relaxation model, by rewriting Gauss law (48) to include the contribution of "fast" polarization processes, $\varepsilon_\infty E$ (ε_∞ = permittivity due to atomic and electronic polarization) whose adaptation to electric field vector E is instantaneous until optical frequencies, and "slow" processes, P_k, which adapt to E according to the Debye generalized equation [123], i.e.,

$$\text{Gauss law} \quad \rho - \nabla \cdot \left(\varepsilon_\infty E + \sum_k P_k \right) = 0 \qquad (55)$$

$$\text{Debyes gener. eq.} \quad \tau_k \partial P_k / \partial t + P_k = \varepsilon_0 \chi_k E. \qquad (56)$$

Numerical simulations in [81] show that, during transients, non-instantaneous polarization processes slow down the electric field dynamics and reduce its maximum intensity.

However, it should be pointed out that neither the more refined calculation methods of transient electric field proposed in [81], [120], and [121], nor the charge carrier injection and transport models for determining localized space charge distributions in HVDC cables proposed in [112], [113], [114], [115], [116], and [117] were used in any life and reliability model for HVDC cable insulation yet. This leaves room to improve the life and reliability modeling of HVDC cables in order to include these methods.

From the above arguments, physical models may seem on the whole superior to phenomenological models, but let us point out that physical models are generally quite complicated [see (1)–(11)] and their parameters are not easy to determine; in fact, the simpler phenomenological models—with parameters derived directly from ALTs—are those used by International Standards for selecting test voltages and durations, and by manufacturers for cable design, as emphasized for model (13) in Section IV-A.

A common limitation of all life and reliability models for HVDC cable insulation is that they hold within the stress range where their parameters were estimated (with some unavoidable uncertainty [17]), as outside such ranges the aging effect of stresses might change and models should be generalized with great care [6], [14], [16]. For instance, the main aging process addressed by each of the physical models (1)–(11) may change and/or be replaced by another mechanism outside the stress range where their parameters were estimated; the value of exponent n in the IPM (13)–(16), of B in the Arrhenius model (17)–(19), of n, B in the related IPM-Arrhenius model (21)–(23), etc., might change when extrapolating these models from the stress levels of ALTs to lower stress levels like the service ones, as pointed out in Section VIII-B when dealing with the TOVs. This is one of the greatest uncertainties faced by life modeling of power system components in general. Luckily the aging rate seems to decrease as stress levels decrease, with a possible tendency to stress thresholds below which insulation life tends to infinity [6], [14], [16], [38]. Then, an extrapolation of life and reliability models from test to service stress levels—as done by International Standards [7], [8], [9], [10], [11], [51]—would be on the safe side. Interesting proposals to account for changes in the electrical aging rate are those found in [49] for the increase of n in the IPM as the field increases, and in [88] for the aging acceleration due to the peak of transient voltage waveforms.

On the other hand, as for the possible change of aging processes from the ALTs to the service stress levels, it is not even strictly necessary for the physical aging mechanism to change with the stress levels. For instance, in [124] it was shown using the physical life model of [41] that the criterion for failure changes from the achievement of a critical field for the onset of a runaway at high applied fields to the link-up of degraded regions at low applied fields.

As a closing remark of this discussion, let us point out that an open issue of life and reliability modeling of HVDC cables is the treatment of accessories. To the author's best knowledge, the only model developed so far to treat a whole HV(dc) cable system including accessories (i.e., joints and terminations) subjected to constant electro-thermal stress is reported in [125]. It was developed from the enlarged electro-thermal reliability model (34) by applying the series reliability (or "weakest link") hypothesis [17], [20] to cable lengths, joints, and terminations composing an HV cable system, and it was used for reliability estimation of HVDC extruded cable systems [125]. However, it has not been cast into a time-varying stress framework yet, although this is one of the goals of the NEWGEN project [5].

X. CONCLUSION

This article has updated a few previous reviews of physical and phenomenological life and reliability models developed over the years for HVDC cable insulation. The update is motivated by the impressive research and development activities on HVDC cable systems in the last years, with many projects at increasing levels of voltage and power, thereby making the sound evaluation of the life and reliability of HVDC cables crucial. As the electric and thermal stresses are always active in power cables, the focus was on such stresses, both constant at rated temperature and voltage and time-varying due to thermal and voltage transients.

The article has discussed the pros and cons of physical versus phenomenological life models. Physical models describe accurately the degradation mechanisms responsible for insulation aging, with parameters attainable from chemical-physical measurements (with no/or limited need for ALTs); this makes them useful for a deeper insight into the behavior of insulating compounds to select the best-performing ones. Phenomenological models are simpler and quite flexible in fitting the results of ALTs, thus in practice, they are preferred for designing and testing HVDC cables, as well as for life and reliability estimation when the electro-thermal stress varies with time, e.g., due to load cycles, or to transient voltage waveforms such as long TOVs, SSIs, and VPRs (all treated in the present review).

The probabilistic framework of electro-thermal life models has also been reviewed, showing how generalized reliability models can be attained to account for the randomness of the electrical breakdown phenomenon, as well as for the decrease of breakdown voltage/field as cable insulation size is enlarged from samples tested in the lab to full-size cables installed in situ.

The limitations and open issues of life and reliability models for HVDC cables have also been highlighted, including the following:

1) The homogeneous insulation hypothesis of phenomenological life models and traditional conductivity-based field calculation methods, which makes them unable to treat localized space charge distributions, local defects, and the effects of slow dipolar polarization processes. Some novel methods for solving these problems have been presented;

2) The inherent uncertainty when extrapolating the models outside their range of validity, pointing out the simple extrapolation done by International Standards using phenomenological models from test to service stresses.

1) The treatment of whole cable systems with cable lengths, joints, and terminations. The detailed treatment of this

open issue has been skipped here for brevity—this is why HVDC cables and not cable systems are mentioned in the title and tackled in the treatment—but it deserves major theoretical developments and nontrivial dedicated tests, since accessories are the weak point of cable systems.

ACKNOWLEDGMENT

REFERENCES

[1] J. C. Fothergill, "The coming of age of HVDC extruded power cables," in *Proc. IEEE Electr. Insul. Conf. (EIC)*, Jun. 2014, pp. 124–137.

[2] G. Mazzanti, "Issues and challenges for HVDC extruded cable systems," *Energies*, vol. 14, no. 15, pp. 1–34, 2021, doi: 10.3390/en14154504.

[3] Federal Network Agency of Germany. *Grid Development Plan 2030 (2019), Second Draft*. Accessed: May 29, 2023. [Online]. Available: https://www.netzentwicklungsplan.de/sites/default/files/paragraphs-files/Standard_presentation_GDP_2030_V2019_2nd_draft.pdf

[4] Wikipedia. *Western HVDC Link*. Accessed: Mar. 21, 2023. [Online]. Available: https://en.wikipedia.org/wiki/Western_HVDC_Link#cite_notewesternhvdclink-mc-4

[5] *CINEA.C—Green Research and Innovation, C.2—Horizon Europe Energy, GRANT AGREEMENT Project 101075592—NEWGEN*, document HORIZON-CL5-2021-D3-02, European Climate, Infrastructure and Environment Executive Agency (CINEA), Brussels, Belgium, Aug. 2022.

[6] G. Mazzanti and M. Marzinotto, *Extruded Cables for High Voltage Direct Current Transmission: Advance in Research and Development*. Hoboken, NJ, USA: Wiley, 2013.

[7] *Recommendations for Testing DC Extruded Cable Systems for Power Transmission at a Rated Voltage up to 500 kV*, document Brochure CIGRÉ 496, Apr. 2012.

[8] *HVDC Power Transmission-Cables with Extruded Insulation and Their Accessories for Rated Voltages up to 320 kV for Land Applications-Test Methods and Requirements*, document IEC 62895, May 2017.

[9] *Recommendations for Testing DC Extruded Cable Systems for Power Transmission At a Rated Voltage Up to and Including 800 kV*, document Brochure CIGRÉ 852, Nov. 2021.

[10] *Recommendations for Testing DC Lapped Cable Systems for Power Transmission At a Rated Voltage Up to and Including 800 kV*, document Brochure CIGRÉ 853, Nov. 2021.

[11] *Power Cables With Extruded Insulation and Their Accessories for Rated Voltages Above 150 kV (Um=170 kV) Up to 500 kV (Um=550 kV) Test Methods and Requirements*, document IEC 62067, 2022.

[12] T. Worzyk, *Submarine Power Cables*. Berlin, Germany: Springer, 2009.

[13] G. C. Montanari and G. Mazzanti, "Insulation aging models," in *Encyclopedia of Electrical and Electronics Engineering*, vol. 10, J. Webster, Ed. New York, NY, USA: Wiley, 1999, pp. 308–319.

[14] G. C. Montanari, G. Mazzanti, and L. Simoni, "Progress in electrothermal life modeling of electrical insulation during the last decades," *IEEE Trans. Dielectr. Electr. Insul.*, vol. 9, no. 5, pp. 730–745, Oct. 2002.

[15] G. Mazzanti and G. C. Montanari, "Electrical aging and life models: The role of space charge," *IEEE Trans. Dielectr. Electr. Insul.*, vol. 12, no. 5, pp. 876–890, Oct. 2005.

[16] G. Mazzanti, "Life and reliability models for high voltage DC extruded cables," *IEEE Electr. Insul. Mag., Special Issue Workshop HVDC cables Accessories*, vol. 33, no. 4, pp. 42–52, Jul./Aug. 2017.

[17] W. Nelson, *Accelerated Testing*. New York, NY, USA: Wiley, 1990.

[18] L. A. Dissado and J. C. Fothergill, *Electrical Degradation and Breakdown in Polymers*. London, U.K.: Peter Peregrinus, 1992.

[19] E. Chiodo and G. Mazzanti, "Theoretical and practical aids for the proper selection of reliability models for power system components," *Int. Jou. Rel. Saf.*, vol. 2, nos. 1–2, pp. 99–128, Oct. 2008.

[20] E. Chiodo and G. Mazzanti, "Mathematical and physical properties of reliability models in view of their application to modern power system components," in *Innovations in Power Systems Reliability*, G. J. Anders and A. Vaccaro, Ed., London, U.K.: Springer, 2011, ch. 3, pp. 59–140.

[21] L. A. Dissado, "Understanding electrical trees in solids: From experiment to theory," *IEEE Trans. Dielectr. Electr. Insul.*, vol. 9, no. 4, pp. 483–497, Aug. 2002.

[22] J. Su, B. Du, J. Li, and Z. Li, "Electrical tree degradation in high-voltage cable insulation: Progress and challenges," *High Voltage*, vol. 5, no. 4, pp. 353–364, Aug. 2020.

[23] G. C. Montanari, "Bringing an insulation to failure: The role of space charge," *IEEE Trans. Dielectr. Electr. Insul.*, vol. 18, no. 2, pp. 339–364, Apr. 2011.

[24] H. A. Alghamdi, G. Chen, and A. Vaughan, "Simulate the effect of trapped charges and trap cross-section on aging process," in *Proc. IEEE Conf. Electr. Insul. Dielectric Phenomena (CEIDP)*, Oct. 2016, pp. 27–30.

[25] J. Ferry, "Experimental methods for viscoelastic liquids," in *Viscoelastic Properties of Polymers*. New York, NY, USA: Wiley, 1961, pp. 82–104.

[26] H. A. Alghamdi and G. Chen, "Relation between trapping parameters and ageing based on a new electro-thermo kinetic equation," in *Proc. IEEE Conf. Electr. Insul. Dielectric Phenomena (CEIDP)*, Oct. 2014, pp. 421–424.

[27] H. Alghamdi, G. Chen, and A. S. Vaughan, "The electro-mechanical effect from charge dynamics on polymeric insulation lifetime," *AIP Advances*, vol. 5, Jun. 2015, Art. no. 127126, doi: 10.1063/1.4939015.

[28] G. C. Montanari and G. Mazzanti, "From thermodynamic to phenomenological multi-stress models for insulating materials without or with evidence of threshold (XLPE cables)," *J. Phys. D, Appl. Phys.*, vol. 27, no. 8, pp. 1691–1702, Aug. 1994, doi: 10.1088/0022-3727/27/8/017.

[29] L. A. Dissado, G. Mazzanti, and G. C. Montanari, "The role of trapped space charges in the electrical aging of insulating materials," *IEEE Trans. Dielectr. Electr. Insul.*, vol. 4, no. 5, pp. 496–506, Oct. 1997.

[30] H. Endicott, B. Hatch, and R. Sohmer, "Application of the Eyring model to capacitor aging data," *IEEE Trans. Compon. Parts*, vol. CP-12, no. 1, pp. 34–41, Mar. 1965.

[31] T. J. Lewis, J. P. Llewellyn, and M. J. Van Der Sluijs, "Electrically induced mechanical strain in insulating dielectrics," in *Proc. IEEE Conf. Electr. Insul. Dielectric Phenomena (CEIDP)*, Oct. 1994, pp. 328–333.

[32] T. J. Lewis, "Ageing—A perspective," *IEEE Electr. Insul. Mag.*, vol. 17, no. 4, pp. 6–16, Jul./Aug. 2001.

[33] T. J. Lewis, "Polyethylene under electric stress," *IEEE Trans. Dielectr. Electr. Insul.*, vol. 9, no. 5, pp. 717–729, Oct. 2002.

[34] J.-P. Crine, "A molecular model to evaluate the impact of aging on space charges in polymer dielectrics," *IEEE Trans. Dielectr. Electr. Insul.*, vol. 4, no. 5, pp. 487–495, Oct. 1997.

[35] J.-P. Crine, "On the interpretation of some electrical aging and relaxation phenomena in solid dielectrics," *IEEE Trans. Dielectr. Electr. Insul.*, vol. 12, no. 6, pp. 1089–1107, Dec. 2005.

[36] L. A. Dissado, G. Mazzanti, and G. C. Montanari, "Elemental strain and trapped space charge in thermoelectrical aging of insulating materials. Part 1: Elemental strain under thermo-electrical-mechanical stress," *IEEE Trans. Dielectr. Electr. Insul.*, vol. 8, no. 6, pp. 959–965, Dec. 2001.

[37] G. Mazzanti, G. C. Montanari, and L. A. Dissado, "Elemental strain and trapped space charge in thermoelectrical aging of insulating materials: Life modeling," *IEEE Trans. Dielectr. Electr. Insul.*, vol. 8, no. 6, pp. 966–971, Dec. 2001.

[38] L. A. Dissado, C. Laurent, G. C. Montanari, and P. H. F. Morshuis, "Demonstrating a threshold for trapped space charge accumulation in solid dielectrics under DC field," *IEEE Trans. Dielectr. Electr. Insul.*, vol. 12, no. 3, pp. 612–620, Jun. 2005.

[39] K. Terashima, H. Sukuki, M. Hara, and K. Watanabe, "Research and development of 250 kV DC XLPE cables," *IEEE Trans. Power Del.*, vol. 13, no. 1, pp. 7–16, Jan. 1998.

[40] E. S. Cooper, L. A. Dissado, and J. C. Fothergill, "Application of thermoelectric aging models to polymeric insulation in cable geometry," *IEEE Trans. Dielectr. Electr. Insul.*, vol. 12, no. 1, pp. 1–10, Feb. 2005.

[41] Z. Zuo, L. A. Dissado, C. Yao, N. M. Chalashkanov, S. J. Dodd, and Y. Gao, "Modeling for life estimation of HVDC cable insulation based on small-size specimens," *IEEE Elect. Insul. Mag.*, vol. 36, no. 1, pp. 19–29, Jan. 2020.

[42] G. Mazzanti, G. Stomeo, and S. Mancini, "State of the art in insulation of gas insulated substations: Main issues, achievements, and trends," *IEEE Elect. Insul. Mag.*, vol. 32, no. 5, pp. 18–31, Sep. 2016.

[43] G. Mazzanti, G. C. Montanari, and F. Civenni, "Model of inception and growth of damage from microvoids in polyethylene-based materials for HVDC Cables. 1. Theoretical approach," *IEEE Trans. Dielectr. Electr. Insul.*, vol. 14, no. 5, pp. 1242–1254, Oct. 2007.

[44] G. Mazzanti, G. C. Montanari, and F. Civenni, "Model of inception and growth of damage from microvoids in polyethylene-based materials for HVDC cables. 2. Parametric investigation and data fitting," *IEEE Trans. Dielectr. Electr. Insul.*, vol. 14, no. 5, pp. 1255–1263, Oct. 2007.

[45] M. Jeroense, "HVDC, the next generation of transmission highlights with focus on extruded cable systems," in *Proc. Int. Symp. Electr. Insulating Mater. (ISEIM)*, Sep. 2008, pp. 10–15.

[46] Y. Maekawa, K. Watanabe, S. Maruyama, Y. Murata, and H. Hirota, "Research and development of DC +/-500 kV extruded cables," in *Proc. CIGR Session*, 2002, pp. 1–8.

[47] S. Nishikawa, K. Sasaki, K. Akita, M. Sakamaki, T. Kazama, and K. Suzuki, "XLPE cable for DC link," *SEI Techn. Rev.*, vol. 84, pp. 59–64, May 2017.

[48] T. Liu et al., "A new method of estimating the inverse power law ageing parameter of XLPE based on step-stress tests," in *Proc. Annu. Rep. Conf. Electr. Insul. Dielectric Phenomena*, Oct. 2013, pp. 69–72.

[49] G. C. Montanari, S. F. Bononi, M. Albertini, S. Siripurapu, and P. Seri, "The dimensional approach in the design and qualification tests of AC and DC HV cables: The Occhini approach revisited," *IEEE Trans. Power Del.*, vol. 35, no. 5, pp. 2119–2126, Oct. 2020.

[50] W. Hauschild and W. Mosch, *Statistical Techniques for High Voltage Engineering*. London, U.K.: Peter Peregrinus, 1992.

[51] *Electrical Insulating Materials—Properties of Thermal Endurance—Part 1: Ageing Procedures and Evaluation of Test Results*, document IEC 60216-1, 2001.

[52] T. W. Dakin, "Electrical insulation deterioration treated as a chemical rate phenomenon," *Trans. Amer. Inst. Electr. Eng.*, vol. 67, no. 1, pp. 113–122, Jan. 1948.

[53] S. Glasstone, K. J. Laidler, and H. E. Eyring, *The Theory of Rate Processes*. New York, NY, USA: McGraw-Hill, 1941.

[54] G. Mazzanti, "Life estimation of HVDC cables under the time-varying electrothermal stress associated with load cycles," *IEEE Trans. Power Del.*, vol. 30, no. 2, pp. 931–939, Apr. 2015.

[55] G. Mazzanti, "Including the calculation of transient electric field in the life estimation of HVDC cables subjected to load cycles," *IEEE Elect. Insul. Mag.*, vol. 34, no. 3, pp. 27–37, May 2018, doi: 10.1109/MEI.2018.8345358.

[56] P. Seri, G. C. Montanari, S. F. Bononi, and M. Albertini, "Comparing the results of increasing-voltage design and qualification life tests on HVDC and HVAC cables: The effect of voltage-step growth rate and insulation thickness factors," in *Proc. IEEE Conf. Electr. Insul. Dielectric Phenomena (CEIDP)*, Oct. 2020, pp. 479–482.

[57] B. Diban and G. Mazzanti, "The effect of temperature and stress coefficients of electrical conductivity on the life of HVDC extruded cable insulation subjected to type test conditions," *IEEE Trans. Dielectr. Electr. Insul.*, vol. 27, no. 4, pp. 1313–1321, Aug. 2020.

[58] *Update of Service Experience of HV Underground and Submarine Cable Systems*, document Brochure CIGRÉ WG B1.57, 2020.

[59] C. Laurent, "Charge dynamics in polymeric materials and its relation to electrical ageing," in *Proc. Annu. Rep. Conf. Electr. Insul. Dielectric Phenomena*, Oct. 2012, pp. 1–20.

[60] H. Yahyaoui et al., "Behavior of XLPE for HVDC cables under thermo-electrical stress: Experimental study and ageing kinetics proposal," *Energies*, vol. 14, no. 21, p. 7344, Nov. 2021.

[61] *Diagnostic and Accelerated Life Endurance Testing of Polymeric Materials for HVDC Application*, document Brochure CIGRÉ 636, version WG D1.23, 2015.

[62] J. M. Oudin, Y. Rerolle, and H. Thevenon, "Theorie statistique du claquage electrique," *Rev. Gen. de L'Electricite*, vol. 77, no. 4, pp. 430–435, 1968.

[63] E. Occhini, "A statistical approach to the discussion of the dielectric strength in electric cables," *IEEE Trans. Power App. Syst.*, vol. PAS-90, no. 6, pp. 2671–2682, Nov. 1971.

[64] D. Fabiani and L. Simoni, "Discussion on application of the Weibull distribution to electrical breakdown of insulating materials," *IEEE Trans. Dielectr. Electr. Insul.*, vol. 12, no. 1, pp. 11–16, Feb. 2005.

[65] S. Sachan, C. Zhou, G. Bevan, and B. Alkali, "Failure prediction of power cables using failure history and operational conditions," in *Proc. IEEE 11th Int. Conf. Properties Appl. Dielectric Mater. (ICPADM)*, Jul. 2015, pp. 380–383.

[66] M. Marzinotto, C. Mazzetti, and G. Mazzanti, "A new approach to the statistical enlargement law for comparing the breakdown performance of power cables. 1. Theory," *IEEE Trans. Dielectr. Electr. Insul.*, vol. 14, no. 5, pp. 1232–1241, Oct. 2007.

[67] M. Marzinotto, C. Mazzetti, and G. Mazzanti, "A new approach to the statistical enlargement law for comparing the breakdown performances of power cables—Part 2: Application," *IEEE Trans. Dielectr. Electr. Insul.*, vol. 15, no. 3, pp. 792–799, Jun. 2008.

[68] M. Marzinotto and G. Mazzanti, "The statistical enlargement law for HVDC cable lines part 1: Theory and application to the enlargement in length," *IEEE Trans. Dielectr. Electr. Insul.*, vol. 22, no. 1, pp. 192–201, Feb. 2015.

[69] M. Marzinotto and G. Mazzanti, "The statistical enlargement law for HVDC cable lines part 2: Application to the enlargement over cable radius," *IEEE Trans. Dielectr. Electr. Insul.*, vol. 22, no. 1, pp. 202–210, Feb. 2015.

[70] M. Marzinotto and G. Mazzanti, "The practical effect of the enlargement law on the electrothermal life model for power-cable lines," *IEEE Elect. Insul. Mag.*, vol. 31, no. 2, pp. 14–22, Mar. 2015.

[71] J. Su, L. Zhao, J. Cheng, P. Yafeng, R. Li, and B. Zeng, "A unified expression for enlargement law on electric breakdown strength of polymers under short pulses: Mechanism and review," *IEEE Trans. Dielectr. Electr. Insul.*, vol. 23, no. 4, pp. 2319–2327, Aug. 2016.

[72] B. Diban and G. Mazzanti, "The effect of insulation characteristics on thermal instability in HVDC extruded cables," *Energies*, vol. 14, no. 3, pp. 1–22, Jan. 2021, doi: 10.3390/en14030550.

[73] G. Mazzanti, "The combination of electro-thermal stress, load cycling and thermal transients and its effects on the life of high voltage AC cables," *IEEE Trans. Dielectr. Electr. Insul.*, vol. 16, no. 4, pp. 1168–1179, Aug. 2009.

[74] *Calculation of the Cyclic and Emergency Current Rating of Cables, Part2: Cyclic Rating of Cables Greater Than 18/30 (36) kV and Emergency Ratings for Cables of All Voltages*, document IEC 60853-2, 1989.

[75] C. K. Eoll, "Theory of stress distribution in insulation of high voltage DC cables. Part I," *IEEE Trans. Electr. Insul.*, vol. EI-10, no. 1, pp. 27–35, Mar. 1975.

[76] M. A. Miner, "Cumulative damage in fatigue," *J. Appl. Mechan.*, vol. 12, pp. A159–A163, Sep. 1945.

[77] C. C. Reddy and T. S. Ramu, "On the intrinsic thermal stability in HVDC cables," *IEEE Trans. Dielectr. Electr. Insul.*, vol. 14, no. 6, pp. 1509–1515, Dec. 2007.

[78] N. Klein, "Electrical breakdown in solids," *Adv. Electr. Electron. Phys.*, vol. 26, pp. 309–424, 1969.

[79] R. N. Hampton, "Some of the considerations for materials operating under high-voltage, direct-current stresses," *IEEE Electr. Insul. Mag.*, vol. 24, no. 1, pp. 5–13, Jan./Feb. 2008.

[80] M. J. P. Jeroense and P. H. F. Morshuis, "Electric fields in HVDC paper-insulated cables," *IEEE Trans. Dielectr. Electr. Insul.*, vol. 5, no. 2, pp. 225–236, Apr. 1998.

[81] P. Cambareri, C. de Falco, L. D. Rienzo, P. Seri, and G. C. Montanari, "Electric field calculation during voltage transients in HVDC cables: Contribution of polarization processes," *IEEE Trans. Power Del.*, vol. 37, no. 6, pp. 5425–5432, Dec. 2022.

[82] *Electric Cables—Calculation of the Current Rating—Part 1–1: Current Rating Equations (100 % Load Factor) and Calculation of Losses—General*, document IEC 60287-1-1, 2006.

[83] *Overvoltages on HVDC Cables*, document JWG 33/21/14.16, 1994.

[84] S. Mukherjee, M. Saltzer, Y.-J. Häfner, and S. Nyberg, "Cable overvoltage for MMC based VSC HVDC system: Interaction with converters," in *Proc. Int. Colloq. HV Insulated Cables*, Oct. 2017, pp. 1–9.

[85] T. Karmokar et al., "Evaluation of 320 kV extruded DC cable system for temporary overvoltages by testing with very long impulse waveform," in *Proc. CIGRÉ Session*, 2018, pp. 1–11.

[86] M. Goertz, S. Wenig, S. Beckler, C. Hirsching, M. Suriyah, and T. Leibfried, "Analysis of cable overvoltages in symmetrical monopolar and rigid bipolar HVDC configuration," *IEEE Trans. Power Del.*, vol. 35, no. 4, pp. 2097–2107, Aug. 2020.

[87] *Surge and Extended Overvoltage Testing of HVDC Cable Systems*, document JWG B4/B1/C4.73, 2023.

[88] G. Mazzanti, "Improved evaluation of the life lost by HVDC extruded cables due to long TOVs," *IEEE Trans. Power Del.*, vol. 37, no. 3, pp. 1906–1915, Jun. 2022.

[89] G. Mazzanti and B. Diban, "The effects of transient overvoltages on the reliability of HVDC extruded cables. Part 1: Long temporary overvoltages," *IEEE Trans. Power Del.*, vol. 36, no. 6, pp. 3784–3794, Dec. 2021.

[90] G. J. Anders and M. A. El-Kady, "Transient ratings of buried power cables. Part I. Historical perspective and mathematical model," *IEEE Trans. Power Del.*, vol. 7, no. 4, pp. 1724–1734, Oct. 1992.

[91] G. Mazzanti and B. Diban, "The effects of transient overvoltages on the reliability of HVDC extruded cables. Part 2: Superimposed switching impulses," *IEEE Trans. Power Del.*, vol. 36, no. 6, pp. 3795–3804, Dec. 2021.

[92] D. Gallo, R. Langella, and A. Testa, "Predicting voltage stress effects on MV/LV components," in *Proc. IEEE Power Tech.*, Jun. 2003, pp. 1–6.

[93] G. Mazzanti, G. Passarelli, A. Russo, and P. Verde, "The effects of voltage waveform factors on cable life estimation using measured distorted voltages," in *Proc. IEEE Power Eng. Soc. Gen. Meeting*, Jun. 2006, pp. 1–8.

[94] G. Mazzanti, P. Seri, B. Diban, and S. Stagni, "Preliminary experimental investigation of the effect of long temporary overvoltages on the reliability of HVDC extruded cables," in *Proc. IEEE 3rd Int. Conf. Dielectr. (ICD)*, Jul. 2020, pp. 49–52.

[95] G. Mazzanti, P. Seri, and B. Diban, "Preliminary experimental investigation of the effect of superimposed switching impulses on XLPE-insulated HVDC cables," in *Proc. IEEE Electr. Insul. Conf. (EIC)*, Jun. 2021, pp. 169–172.

[96] X. Wang, Q. Jiang, C. Wu, S. Liu, and K. Wu, "Study on space charge characteristics in XLPE under DC voltage superimposed by impulse voltage," *IEEE Trans. Dielectr. Electr. Insul.*, vol. 30, no. 1, pp. 184–192, Feb. 2023.

[97] A. Battaglia, M. Marzinotto, and G. Mazzanti, "A deeper insight in predicting the effect of voltage polarity reversal on HVDC cables," in *Proc. IEEE Conf. Electr. Insul. Dielectric Phenomena (CEIDP)*, Oct. 2019, pp. 442–445.

[98] *DC Cable Systems With Extruded Dielectrics*, EPRI document 1008720, Palo Alto, CA, USA, Dec. 2004.

[99] A. Cavallini, D. Fabiani, G. Mazzanti, and G. C. Montanari, "Life model based on space-charge quantities for HVDC polymeric cables subjected to voltage-polarity inversions," *IEEE Trans. Dielectr. Electr. Insul.*, vol. 9, no. 4, pp. 514–523, Aug. 2002.

[100] G. Mazzanti, M. Marzinotto, and A. Battaglia, "A first step towards predicting the life of HVDC cables subjected to load cycles and voltage polarity reversal," in *Proc. IEEE Conf. Electr. Insul. Dielectric Phenomena (CEIDP)*, Oct. 2015, pp. 783–786.

[101] B. Diban, G. Mazzanti, M. Marzinotto, and A. Battaglia, "Calculation of electric field profile within HVDC cable insulation in the presence of voltage polarity reversals," in *Proc. IEEE 4th Int. Conf. Dielectr. (ICD)*, Jul. 2022, pp. 13–16.

[102] T. T. Nga Vu, G. Teyssedre, and S. L. Roy, "Electric field distribution in HVDC cable joint in non-stationary conditions," *Energies*, vol. 14, no. 5401, pp. 1–17, Aug. 2021.

[103] M. Tefferi, Z. Li, H. Uehara, Q. Chen, and Y. Cao, "Characterization of space charge and DC field distribution in XLPE and EPR during voltage polarity reversal with thermal gradient," in *Proc. IEEE Conf. Electr. Insul. Dielectric Phenomenon (CEIDP)*, Oct. 2017, pp. 617–620.

[104] G. Rizzo et al., "Polarity reversal in HVDC joints—The effect of the axial thermal conduction," in *Proc. IEEE Conf. Electr. Insul. Dielectric Phenomena (CEIDP)*, Oct. 2020, pp. 115–118.

[105] S. Dhayalan, A. Das, P. Johri, and C. C. Reddy, "Estimation of electric field and temperature in HVDC cables under different environmental conditions," in *Proc. IEEE 16th Int. Conf. Ind. Inf. Syst. (ICIIS)*, Dec. 2021, pp. 262–264.

[106] Z. Zuo, L. A. Dissado, C. Yao, N. M. Chalashkanov, S. J. Dodd, and Y. Gao, "Emergent failure patterns at sub-critical fields in polymeric dielectrics," *J. Mater. Sci.*, vol. 55, no. 11, pp. 4748–4761, Apr. 2020.

[107] C. O. Olsson and M. Jeroense, "Evolution of the distributions of electric field and of space charge in an extruded HVDC cable," in *Proc. Int. Conf. Insul. Power Cables (Jicable)*, Jun. 2011, pp. 19–23.

[108] T. Takada, "Acoustic and optical methods for measuring electric charge distributions in dielectrics," *IEEE Trans. Dielectr. Electr. Insul.*, vol. 6, no. 5, pp. 519–547, Dec. 1999.

[109] A. Imburgia, R. Miceli, E. R. Sanseverino, P. Romano, and F. Viola, "Review of space charge measurement systems: Acoustic, thermal and optical methods," *IEEE Trans. Dielectr. Electr. Insul.*, vol. 23, no. 5, pp. 3126–3142, Oct. 2016.

[110] G. Teyssedre and C. Laurent, "Charge transport modeling in insulating polymers: From molecular to macroscopic scale," *IEEE Trans. Dielectr. Electr. Insul.*, vol. 12, no. 5, pp. 857–875, Oct. 2005.

[111] T. Katayama, T. Yamazaki, Y. Murata, S. Mashio, and T. Igi, "Space charge characteristics in DC-XLPE cable after 400 kV PQ test," in *Proc. Int. Conf. Insul. Power Cables (Jicable)*, Jun. 2015, pp. 1–6.

[112] F. Baudoin, S. Le Roy, G. Teyssedre, and C. Laurent, "Bipolar charge transport model with trapping and recombination: An analyze of the current vs. applied electric field characteristic," in *Proc. IEEE Int. Conf. Solid Dielectr.*, Jul. 2007, pp. 19–22.

[113] S. Le Roy, "Numerical methods in the simulation of charge transport in solid dielectrics," *IEEE Trans. Dielectr. Electr. Insul.*, vol. 13, no. 2, pp. 239–246, Apr. 2006.

[114] S. Le Roy, G. Teyssèdre, and C. Laurent, "Modelling space charge in a cable geometry," *IEEE Trans. Dielectr. Electr. Insul.*, vol. 23, no. 4, pp. 2361–2367, Aug. 2016.

[115] Y. Zhan, G. Chen, and M. Hao, "Space charge modelling in HVDC extruded cable insulation," *IEEE Trans. Dielectr. Electr. Insul.*, vol. 26, no. 1, pp. 43–50, Feb. 2019.

[116] Y. Zhan et al., "Space charge measurement and modelling in cross-linked polyethylene," *Energies*, vol. 13, no. 8, p. 1906, Apr. 2020.

[117] Y. Zhan et al., "Comparison of two models on simulating electric field in HVDC cable insulation," *IEEE Trans. Dielectr. Electr. Insul.*, vol. 26, no. 4, pp. 1107–1115, Aug. 2019.

[118] E. Ildstad, J. Sletbak, B. R. Nyberg, and J. E. Larsen, "Factors affecting the choice of insulation system for extruded HVDC power cables," in *Proc. CIGRE Session*, 2004, pp. 1–8.

[119] *Recommended Practice for Space Charge Measurements in HVDC Extruded Cables for Rated Voltages up to 550 kV*, IEEE Standard 1732–2017, Jun. 2017.

[120] H. Naderiallaf, P. Seri, and G. C. Montanari, "Designing a HVDC insulation system to endure electrical and thermal stresses under operation. Part I: Partial discharge magnitude and repetition rate during transients and in DC steady state," *IEEE Access*, vol. 9, pp. 35730–35739, 2021.

[121] H. Naderiallaf, P. Seri, and G. C. Montanari, "Effect of voltage slew rate on partial discharge phenomenology during voltage transient in HVDC insulation: The case of polymeric cables," *IEEE Trans. Dielectr. Electr. Insul.*, vol. 29, no. 1, pp. 215–222, Feb. 2022.

[122] T. Sörqvist, T. Christen, M. Jeroense, V. Mondiet, and R. Papazyan, "HVDC light cable systems-highlighting the accessories," in *Proc. Nordic Insul. Symp. (NORDIS)*, Jun. 2009, pp. 1–6.

[123] A. K. Jonscher, *Dielectric Relaxation in Solids*. London, U.K.: Chelsea Dielectric Press, 1983.

[124] L. A. Dissado, "The theory of everything in the electrical breakdown of polymeric dielectrics: Maybe," in *Proc. IEEE 2nd Int. Conf. Dielectr. (ICD)*, Jul. 2018, pp. 1–5, doi: 10.1109/ICD.2018.8468402.

[125] G. Mazzanti and M. Marzinotto, "Advanced electro-thermal life and reliability model for high voltage cable systems including accessories," *IEEE Elect. Insul. Mag.*, vol. 33, no. 3, pp. 17–25, May 2017.

Giovanni Mazzanti (Fellow, IEEE) is currently an Associate Professor of HV engineering and power quality with the University of Bologna, Bologna, Italy. He is a Consultant with TERNA (the Italian TSO), Rome, Italy. He has authored or coauthored more than 300 published papers, and a book titled *Extruded Cables for HVDC Transmission: Advances in Research and Development* (Wiley-IEEE Press, 2013). His research interests are reliability and diagnostics of HV insulation, power quality, renewables, and human exposure to electro-magnetic fields (EMF).

Mr. Mazzanti is a member of IEEE Power and Energy Society (PES) and Dielectrics and Electrical Insulation Society (DEIS), IEEE DEIS Technical Committee (TC) on "Smart Grids," International Electrotechnical Commission (IEC), Conference International des Grands Reseaux Electriques (CIGRÉ), CIGRÉ Joint Working Group B4/B1/C4.73 on "Surge and Extended Overvoltage Testing of High Voltage Direct-Current (HVDC) cable systems." He is the Chair of the IEEE DEIS TC on "HVDC Cable Systems" and responsible for the University of Bologna research team in the EU H-2020 NEWGEN project.